EFFECT OF BALL SIZE DISTRIBUTION ON MILLING PARAMETERS

François Mulenga Katubilwa

A dissertation submitted to the Faculty of Engineering and the Built Environment, University of the Witwatersrand, in fulfilment of the requirements for the degree of Master of Science in Engineering

Johannesburg, 2008

I declare that this dissertation is my own unaided work. It is being submitted for the Degree of Master of Science in Engineering to the University of the Witwatersrand, Johannesburg. It has not been submitted before for any degree or examination to any other University.

François Mulenga Katubilwa

23rd day of September 2009

Abstract

This dissertation focuses on the determination of the selection function parameters α, a, μ, and Λ together with the exponent factors η and ξ describing the effect of ball size on milling rate for a South African coal.

A series of batch grinding tests were carried out using three loads of single size media, i.e. 30.6 mm, 38.8 mm, and 49.2 mm. Then two ball mixtures were successively considered. The equilibrium ball mixture was used to investigate the effect of ball size distribution on the selection function whereas the original equipment manufacturer recommended ball mixture was used to validate the model.

Results show that with the six parameters abovementioned estimated, the charge mixture is fully characterized with about 5 – 10 % deviation. Finally, the estimated parameters can be used with confidence in the simulator model allowing one to find the optimal ball charge distribution for a set of operational constraints.

To my lovely family

My parents François-Xavier Kabeke and Bernadette Kabeke

My sisters Linda Kabeke and Arlette Kabeke

My brother Pacha Kabeke

My nephew Noam Mulenga

François M. Katubilwa

Acknowledgements

First and foremost, praise to the Almighty GOD who gave me the opportunity to do a Master's project. My Lord Jehovah Jireh has always been there to support, guide, encourage and strengthen me in each and every step of this project.

Secondly, I thank the supervisor of my Master of Science Dissertation, Professor Michael Moys. His valuable advices, assistance in proof-reading the draft of the dissertation, and availability in orientating me when things could not break through are highly appreciated.

Thirdly, I present my gratitude to all the individuals that have unconditionally assisted and helped me in any way during my research. Dr Murray Bwalya and Mr. Gerard Finnie are acknowledged for the multiple advices and suggestions during the data analysis process of the laboratory results. Mr. Daniel Mokhathi is also acknowledged for his help in the laboratory. I will always be grateful towards them. My sincere wish is to see them continuing to corporate well with other people like they did with me.

Thanks are also due to Pascal Simba, Allan Chansa, Crispin Kilumba and his entire family for the moral support throughout this experience of life.

Lastly, I would like to thank the Centre of Material and Process Synthesis of the University of the Witwatersrand, Eskom and the National Research Funds of South Africa for funding this work and allowing the publication of the results.

Katubilwa, F.M.

Table of contents **Page**

List of figures

List of tables

Table **Page**

List of symbols

a or $a(d)$	Parameter characteristic of the material
A	Material-dependent constants in Equations (2.16) and (2.17)
A'	Material-dependent constants in Equations (2.16) and (2.17)
A^o	Material dependent constant in Equation (2.12)
A_r	Constant showing the material strength
B	Material-dependent constants in Equations (2.16) and (2.17)
B'	Material-dependent constants in Equations (2.16) and (2.17)
b'_{ii}	Parameter defined in Equations (2.23) and (2.24)
$b_{i,j}$	Mass fraction arriving in size interval i from breakage of size interval j
$\bar{b}_{i,j}$	Mean breakage function of particles of size j breaking into size i corresponding to a ball mixture
$b_{i,j,k}$	Fractional breakage into size i from breakage of size j by size k balls
$B_{i,j}$	Cumulative breakage function of particles of size x_j into size x_i
c	Constant deduced from experimental data in Equation (2.15)
C'	Proportionality constant in Equation (2.13)
C_1	Constant as defined in Equation (2.19)
C'_1	Constant as defined in Equation (2.20)
C_2	Constant as defined in Equation (2.19)
C'_2	Constant as defined in Equation (2.20)
d	Ball diameter
d_k	Diameter of balls in the makeup
$d_{\min}$	Diameter of the ball leaving the mill after being worn down
$d_{\max}$	Maximum diameter of ball in the charge

d^o	Material dependent constant in Equation (2.12)
f_c	Fraction of mill volume occupied by the bulk volume of powder charged
k	Wear law constant whose dimensions depend on the value of Δ in Equation (2.27)
k_1	Constant which represents rate of change of radius in Bond wear law
K	Maximum breakage rate factor
m	Constant as defined in Equation (2.19)
M_b	Mass of a ball
m_k	Weight fraction of balls in class size k, relative mass frequency function of balls of size d_k
m_0^{I}	Relative number frequency of balls in the makeup
$m(t)$ or $m_i(t)$	Mass fraction of particles of size i at time t
M_3^{ss}	Cumulative mass distribution of balls at steady-state
n	Number of ball sizes
n_0	Constant as defined in Equation (2.19)
$\overline{N}(d)$	Fraction by number of media with radii greater than d
p	Number of ball classes in the makeup
$P_c(x)$	Probability of crushing a particle of size x nipped by two colliding balls
$P_{expt}(t)$	Retained mass fraction on top size screen x at grinding time t as experimentally measured
$P_i(t)$	Weight fraction of the material less than size x_i at time t
$P_{model}(t)$	Predicted mass fraction retained on size screen x after grinding of single-sized material of initial size x for a total grinding time t
$P_n(x)$	Probability of nipping a particle of size x by two approaching balls

$q(x)$	Function describing the probability of crushing nipped particles
$Q(x)$ or $Q(x_i)$	Correction factor of the selection function equation in the abnormal breakage region
r_b	Ball radius
r^2	Coefficient of determination also called R-squared value
R	Total number of runs required to carry out a full batch test on a given particle size x
s_e	Standard error of estimate
S_i or $S_i(d)$	Rate of disappearance of material of size i or specific rate of breakage of particles of size x_i, also known as selection function
$S_{i,k}$ or $S_i(d_k)$	Selection function of particle size x_i due to balls of size d_k
S_m	Maximum value of the selection function for given ball and mill diameters
$\overline{S}$	Weighted mean value of S_i for the mixture of ball sizes in the mill
SSE	Objective function defined as the Sum of Squared Errors
t	Time defined for the grinding process or the wear mechanism
x_i	Size of particles in class i; for a size interval the upper size used to represent the particle size
x_m	Particle size for which S_i is maximum for given ball and mill diameters
U	Unit step function
V_G	Volume of the zone of possible nipping in the grinding zone
V_M	Mill volume
V_r	Mean relative velocity of ball
$w_i(t)$	Mass fraction of unbroken material of size i in the mill at time t
Z_{ef}	Frequency of collisions effective for crushing
α	Parameter characteristic of the material
β	Breakage parameter characteristic of the material used whose values range from 2.5 to 5

β_G	Material dependent constant in Equation (2.12)
β_N	Constant independent of material and operational conditions
γ	Breakage parameter characteristic of the material whose values typically are found to be between 0.5 and 1.5
γ_G	Material dependent constant in Equation (2.12)
Δ	Wear rate factor defining the ball wear law
ε_p	Void fraction of the static bed in a tumbling ball mill
η	Exponent factor in Equation (2.11)
η_N	Constant independent of material and operational conditions
ξ	Exponent factor in Equation (2.10)
λ	Average ball-ball distance in the grinding zone. It has been shown to vary with mill operating conditions
Λ	Positive number representing an index of how rapidly the rate of breakage falls as size increases in the abnormal region
μ or $\mu(d)$	Particle size at which the correction factor $Q(x)$ is 0.5 for a ball diameter d, it varies with mill conditions
ϕ_i	Fraction of slow-breaking material in Equations (2.23) and (4.2)
Φ_j	Breakage parameter characteristic of the material used, it represents the fraction of fines that are produced in a single fracture event
τ	Maximum life of the media in the mill due to wear

Chapter 1 Introduction

1.1 Background

For many decades milling has been the subject of intensive research. Describing and understanding the process has been challenging because of the chaotic environment of the tumbling mill itself. Mathematical models obtained so far are mainly based on a mechanistic approach of the phenomenon. Despite the limitation of these models, results produced have proven to be satisfactorily to a great extent.

As far as reliability and mechanical efficiency are concerned, tumbling ball mills are the preferred choice for size reduction.

The problem with tumbling ball mills is that they are extremely wasteful in terms of energy consumed (Wills, 1992). Therefore, the benefit of describing as accurately as possible the grinding environment will not only help better understand the process itself but also improve the use of available energy.

In order to do so, several factors influencing the process are to be considered. Certainly, the starting point would be some investigation of the mill load behaviour since it plays a paramount role in the overall grinding mechanism.

The major factors directly influencing the load behaviour are the constitution of the charge, the speed of rotation of the mill, and the type of motion of individual pieces of medium in the mill (Gupta and Yan, 2006). Mill speed and liner profile are generally fixed operating parameters considering the fact that liners wear very slowly. As a result, the type of motion of particles does not change on average. This implies on an industrial point of view that flexibility will be most of the time limited only to the constitution of the charge.

Concha *et al.* (1992) were able to get a 12% increase in capacity of an industrial mill circuit by systematically optimizing the ball charge mixture. Hence, particular attention should be paid to making sure that the charge is sensibly controlled. For this reason, a clear description of the effect of mill load composition will allow one to better model the grinding process and thereby provide a tool to find possible increases in mill performance.

1.2 Statement of the problem

Coal is one of the most important commodities of South Africa. The mineral industry and energy production sector are highly dependent on it. In the country, it is the primary source used in the production of energy for mining industry and miscellaneous needs. Basically, coal is mined, then pulverized and finally send to the boiler for electricity production.

Coalfields on the planet are divided into two broad regions: the Gondwana and the Laurasia. The Gondwana region refers to coals that are found mainly in the Southern hemisphere. It includes Southern African coals, as well as those in India, Australia, and South America. The Laurasian region on the contrary includes the carboniferous coals found in the northern hemisphere.

In general, coals of the Gondwanaland have been found to be highly variable in rank (maturity) and organic-matter composition compared to their counterparts in the Laurasia. The major differences between the Carboniferous coals of the northern hemisphere, and those found in the southern hemisphere reside in their respective petrographic properties.

Falcon and Falcon (1987) have investigated the effects of this differentiation on the combustion performance of coal. They showed that the petrographic characteristics (i.e. organic composition and rank) of coals play a very important role in combustion behaviour. The study also revealed dramatic differences between northern and southern coals in terms of combustion characteristics. In this regard, the rank of coal that defines the degree of transformation undergone by the seam through the processes of time, temperature, or pressure in the in-depth rock mass could also influence the mechanical properties of coal.

Later on, Falcon and Ham (1988) reported that except for the South Rand and Orange Free State Coalfields, the European coals are in general much easier to grind than those of Southern Africa.

The presence of syngenetic mineral matters (as opposed to secondary or epigenetic minerals filling cracks or fissures) disseminated in the matrix is believed to increase the strength of southern coals (Falcon and Falcon, 1987). This is due to the fact that syngenetic mineral matters are formed at the same time as the enclosing rock and therefore make the deposit to be more compact. Epigenetic minerals, on the other hand, are formed after the enclosing rock has been formed.

Published results of laboratory tests on coal for comminution purposes have reported findings that would be applicable specifically to the Laurasian coals (Austin *et al.*, 1984).

Because of the very limited information available on the South African coals, many of the grinding parameters obtained on other coals have been used as default values. However, coal properties vary markedly amongst seams, coalfields, and regions of the world. Now, the question is: Is it sensible to consider South African coals to be similar to Laurasian ones in terms of grinding performance?

1.3 Research objective

The well accepted Population Balance Model requires for its use a complete breakage characterization of the material being described in terms of selection and breakage functions. In order to achieve this, a series of laboratory tests need to be carried out on a material sample under consideration.

In the present dissertation the applicability of the population balance model on a South African coal is addressed. Some breakage parameters are reviewed to find suitable values for South African coals. Specifically, the breakage kinetics of coal in relation to the diameter of grinding media is studied. The aim is to fix definitely the basis for breakage parameter estimation of South African coals in general. By the same token, an attempt to clarify some issues pertaining to the effect of ball diameter on milling rate. Then, the effect of ball mixture on the breakage rate parameters of coal is assessed to provide valuable information for the simulation of industrial mills used in Eskom Power Stations. Focus is allocated only on the dependence of the selection function with respect to ball charge composition in the mill.

Discussion of the influence of the petrographic properties of coal on breakage will not be touch upon as it is beyond the scope of this dissertation. Such a question remains to be extended for more detailed consideration. Moreover, the characterization of breakage properties of coal will be limited to the feed coal generally used at Tutuka Power station.

1.4 Layout of the dissertation

The dissertation is organized into six chapters with the first chapter being the introduction. The second chapter presents a summary of relevant theory of milling. The state of current knowledge is reviewed with emphasis on the effect of ball size and ball size distribution on milling rate. In addition, the dependency between the competent ball diameter needed to optimally break a coal particle of given size is discussed.

The third chapter provides a detailed description of the laboratory work and equipment used to achieve the objective. Different procedures, the experiment design, and laboratory work involved are presented.

The fourth chapter aims at characterizing a South African coal in terms of breakage kinetics. After collection of data from the Wits pilot mill, the necessary information on the grinding process is compiled. This information is crucial for scale-up and simulation purposes in future works.

The fifth chapter presents the effect of ball size distribution on milling parameters for simulation of industrial cases. It provides a better understanding of this effect and attempt to validate available models for scale-up purposes in Eskom plants.

The last chapter gives a summary of the important findings, their relevance, and some recommendations for future investigation.

Chapter 2 Literature Review

2.1 Introduction

For many decades milling has been dealt with as a black box. In this technique, a single operation is reduced to a box with an input and an output. Then, the mill product size is estimated as a function of size and hardness of the mill feed, and milling operating conditions (Napier-Munn *et al.*, 1996).

A more realistic approach is the so-called Population Balance Model. In this approach, the full description of the process reduces to two key components, namely the Selection function and the Breakage function. Using these two functions simple mass balances are constructed for each size fraction and following this the overall operation is modelled.

A summary of the key elements describing the population balance model is presented in this chapter, that is, selection and breakage functions. The interdependence between these functions and mill conditions, specifically the size of the grinding media and the ball size distribution of the charge, is also discussed.

2.2 Breakage mechanism in tumbling ball mills

Several mechanisms contribute to the grinding action that takes place inside a mill. These include impact or compression, chipping, and abrasion. These mechanisms deform particles beyond their limits of elasticity and cause them to break (Wills, 1992).

The relative motion between media is responsible to a great extent for the grinding action. Ball media are entrained in a tumbling motion which engenders some interactions. During these interactions media collide or roll over each other. Depending on the type and the magnitude of the interaction, particles break following a certain pattern. King (2001) argued that in a ball mill particles break primarily by impact or crushing and attrition. It seems however that impact breakage is predominant at coarser particle sizes whilst attrition is the main reduction mechanism at finer sizes. In between the two extremes, breakage is composed of some combination of impact and abrasion. For the purpose of this dissertation breakage is considered to be a result of impact, abrasion, and attrition only. Other types of breakage mechanisms are not discussed here.

2.2.1 Impact breakage

Breakage by impact occurs when forces are normally applied to the particle surface. It is also referred to as breakage by compression. King (2001) expounded this mechanism of fracture and showed that it encompasses shatter and cleavage.

Fracture by cleavage occurs when the energy applied is just sufficient to load comparatively few regions of the particle to the fracture point, and only a few particles result. The progeny size is comparatively close to the original particle size. This type of fracture occurs under conditions of slow compression where the fracture immediately relieves the loading on the particle. Fracture by shatter on the other hand occurs when the applied energy is well in excess of that required for fracture. Under these conditions many areas in the particle are over-loaded and the result is a comparatively large number of particles with a wide spectrum of sizes. This occurs under conditions of rapid loading such as in a high velocity impact (Kelly and Spottiswood, 1982).

2.2.2 Abrasion breakage

Abrasion is seen as a surface phenomenon which takes place when two particles move parallel to their plane of contact. Small pieces of each particle are broken or torn out of the surface, leaving the parent particles largely intact. Abrasion fracture occurs when insufficient energy is applied to cause significant fracture of the particle. Rather, localized stressing occurs and a small area is fractured to give a distribution of very fine particles (effectively localized shatter fracture) (Kelly and Spottiswood, 1982).

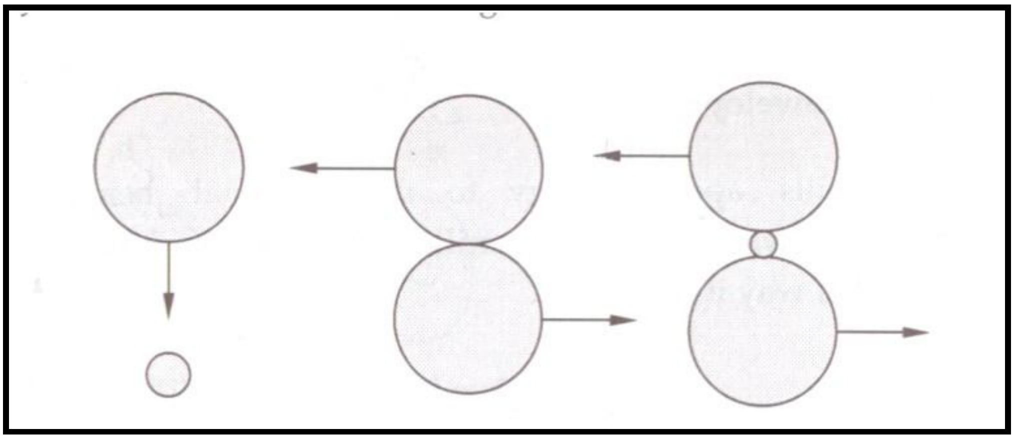

Figure 2.1 Breakage mechanisms in a ball mill (Napier-Munn *et al.*, 1996)

2.2.3 Breakage by attrition

When a ball mill is running at low speed, grinding is a result of rubbing action within the ball mass and between the ball mass and the mill liners. The size reduction depends mainly on the surface areas of the media in interaction (Hukki, 1954). This breakage mechanism is known as attrition. It is caused by the relative movement between powder and individual grinding media components in the mill.

In the relative motion of particles and media, very small particles happen to be nipped between large balls or between large balls and mill liners. The rubbing together of the two media or of media and liners will result in the production of a significant number of very fine particles compared to the parent size. For that reason, it would be fair to assume that attrition is largely responsible for the breaking of particles that have become smaller than the voids between the grinding media and that the stresses induced in the particle nipped between the two media or between the media and the liners are not large enough to cause fracture (King, 2001).

2.3 Population balance model

The objective of any operation of size reduction is to break large particles down to the required size. In tumbling ball mills for instance, this operation is achieved through repetitive actions of breakage. Modelling such a mechanism necessitates a detailed understanding of the grinding process itself. Then, allowing for all the operating variables and machine characteristics the feed and product size distributions can be related.

Fragments from each particle that appear after first breakage consist of a wide range of particle sizes. Some of the daughter fragments are still coarse and require further breakage. The probability of further breakage depends on the machine design and particle size.

The underlying physics suggests that the process is apparently a combination of two actions taking place simultaneously inside the mill: a selection of the particle for breakage, and a breakage resulting in a particular distribution of fragment sizes after the particle is selected (Gupta and Yan, 2006). A size-mass balance inside the mill that takes into account the two abovementioned reactions will make full description of the grinding process possible. And eventually, mathematical relations between feed size and product size, after comminution, can be developed.

2.3.1 Selection function

The disappearance of particles per unit time and unit mass due to breakage is assumed to be proportional to the instantaneous mass fraction of particles of that size fraction present inside the mill. This statement known as the first-order breakage hypothesis is written as follows:

$$\frac{dw_i(t)}{dt} = -S_i w_i(t) \qquad (2.1)$$

where $w_i(t)$ represents the mass fraction of unbroken material of size i in the mill at time t

S_i is the rate of disappearance of material of size i, also known as selection function.

Because the population balance model is based upon the first order grinding law it is sometimes referred to as the "first order rate model" (Napier-Munn *et al.*, 1996).
It is not yet established in theory why particles follow this law. Despite its simplicity the law has proven to apply to numerous materials so far especially for fine sizes. Research is currently being conducted in order to get much insight in the foundation of this assumption. But until that is achieved, the model is reasonably good for many materials over a wide range of operation (Austin *et al.*, 1984; Napier-Munn *et al.*, 1996).

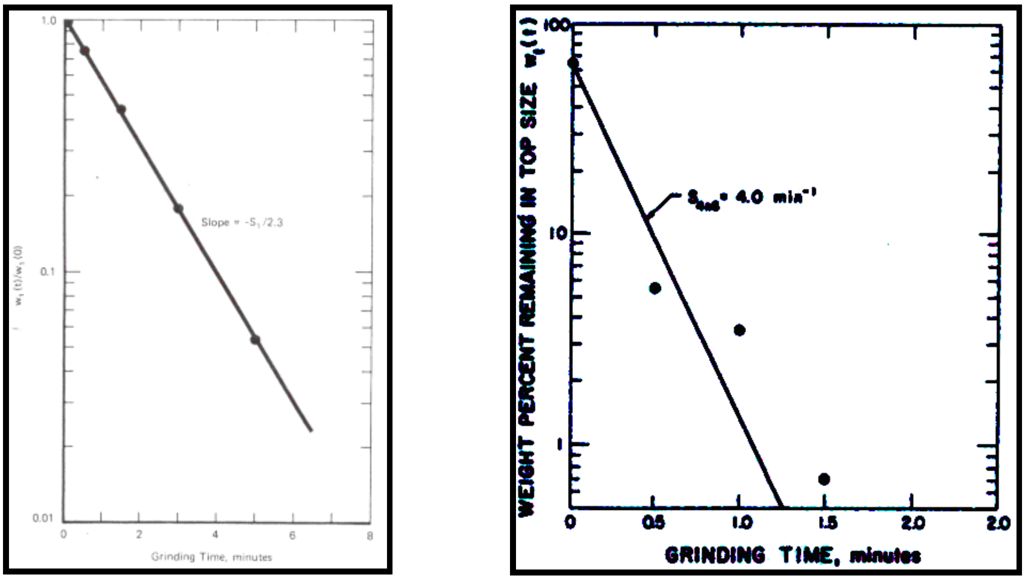

Figure 2.2 First order reaction model applied to milling after Austin *et al.* (1984)
(a) Normal breakage; (b) Abnormal breakage

Figure 2.2(a) shows the first-order breakage law for a given material. However, substantial deviations from the first-order law are noted for coarse materials (Austin *et al.*, 1973). In this case breakage is said to occur in the abnormal region and is illustrated in Figure 2.2(b). This behaviour is addressed later in this dissertation.

Perhaps the most important point is how the rate of breakage changes with respect to particle size. According to Griffith theory of breakage (Austin *et al.*, 1984), for the same size of balls in a mill, very fine particles are hard to break. This suggests that as the particle size increases the breakage rate should continuously increase. The general observed trendline (Figure 2.3) agrees consistently with this statement. But then comes a turning point after which particles become too large to be nipped by balls. The rate of breakage steadily drops and tends to zero.

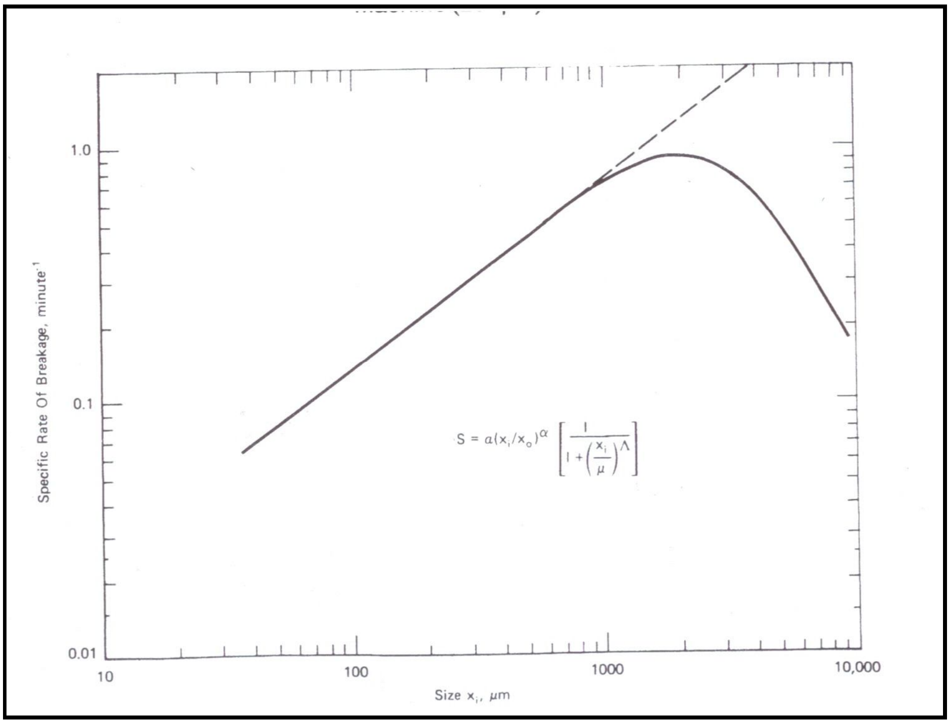

Figure 2.3 Grinding rate versus particle size for a given ball diameter (Austin *et al.*, 1984)

Now, based on the results of several laboratory tests, Austin *et al.* (1984) were able to show that the rate of disappearance of particles as a function of size is given by

$$S_i = a.x_i^\alpha.Q(x_i) = a.x_i^\alpha \frac{1}{1+\left(\frac{x_i}{\mu}\right)^\Lambda} \tag{2.2}$$

where x_i is the particle size in class i in mm

α and a are parameters strongly dependent on the material used

μ defines the particle size at which $Q(x_i)$=0.5, it varies with mill conditions

Λ is an index allowing for the decrease in the value of the selection function with increasing particle size

For finer materials, it is readily seen that $Q(x)$ reduces to approximately 1, and therefore Equation (2.2) becomes $S_i = a.x_i^{\alpha}$. The reduced equation geometrically represents on log-log scale a straight line of which characteristics are the slope α (see dotted line in Figure 2.3) and the breakage rate a at a standard particle size here taken as 1 mm.

The parameter α is a positive number normally in the range 0.5 to 1.5. It is characteristic of the material and does not vary with rotational speed, ball load, ball size or mill hold-up over the normal recommended test ranges (Austin and Brame, 1983) for dry milling, but the value of a will vary with mill conditions.

In the correction factor $Q(x)$, Λ is a positive number which is an index of how rapidly the rates of breakage fall as size increases: The higher the value of Λ, the more rapidly the values decrease. The parameter Λ is found to be primarily a characteristic of the material.

2.3.2 Breakage function

The breakage function, better called the primary breakage distribution function, can be defined as the average size distribution resulting from the fracture of a single particle (Kelly and Spottiswood, 1990).

After a single step of breakage of a particle, the distribution of sizes produced is described in terms of breakage or appearance function. Thus the relative distribution of each size fraction after breakage is perceived as a full description of the product. That is why the primary breakage distribution function of a particle of size j to size i is defined as follows:

$$b_{i,j} = \frac{mass\ of\ \ particles\ \ from\ class\ \ j\ broken\ to\ size\ i}{mass\ of\ \ particles\ of\ \ class\ \ j\ broken} \tag{2.3}$$

A more convenient way of describing the breakage distribution function is to use the cumulative breakage function defined as follows (Austin *et al.*, 1984):

$$B_{i,j} = \sum_{k=n}^{i} b_{k,j} \tag{2.4}$$

Using this new definition of the breakage distribution function, the general fitting model of the cumulative breakage function for a non-normalizable material can be expressed as follows

$$B_{i,j} = \Phi_j \left(\frac{x_{i-1}}{x_j} \right)^{\gamma} + \left(1 - \Phi_j\right) \left(\frac{x_{i-1}}{x_j} \right)^{\beta} \tag{2.5}$$

where β is a parameter characteristic of the material used whose values range from 2.5 to 5

γ is also a material-dependent characteristic whose values typically are found to be between 0.5 and 1.5

Φ_j represents the fraction of fines that are produced in a single fracture event. It is also dependent on the material used.

Equation (2.5) represents an empirical model relating the cumulative breakage function to the particle size and is plotted in Figure 2.4.

A simple but effective assumption is to consider the breakage distribution function as independent of the initial particle size. In other words, the breakage function is assumed to be normalizable. In this case, Φ_j is not a function of the parent size *j*. Though arguable in essence, this assumption has proven to be reasonable for many materials.

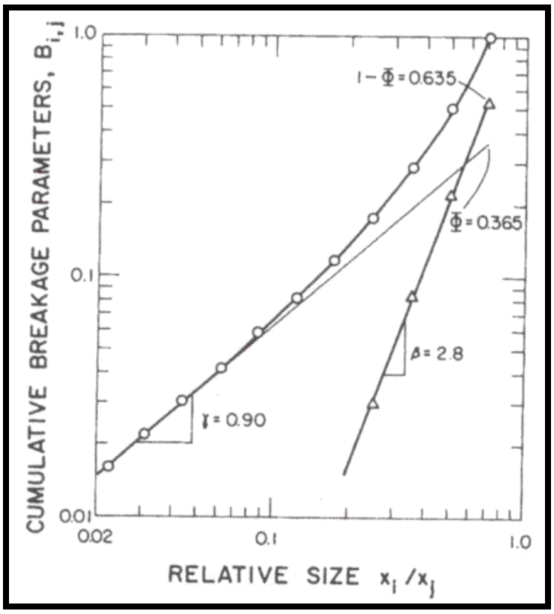

Figure 2.4 Cumulative breakage function versus relative size (Austin *et al.*, 1984)

2.3.3 Batch grinding equation

The kinetics of breakage is most of the time investigated by means of batch grinding tests. A series of laboratory tests in a small mill are performed using a procedure known as the one-size-fraction method (Austin *et al.*, 1984). A sample in one size class is prepared. Then, the material is loaded in the mill together with the ball media. Grinding is performed for several suitable grinding time intervals. After each interval, the product is sieved. Thus the disappearance rate of feed size material is monitored for the different grinding time intervals.

Lastly, the material is characterized in terms of breakage rate and breakage function.

Using the breakage characteristics of the material, a size-mass balance is performed for each size interval. Basically, the amount of material being broken into and out of the size interval of interest, and the starting feed mass are simultaneously considered around the size of interest. This is symbolically expressed in the following equation (Austin and Bhatia, 1971/72):

$$\frac{dw_i(t)}{dt} = -S_i w_i(t) + \sum_{j=1}^{i-1} b_{i,j} S_j w_j(t) \tag{2.6}$$

where S_i is the selection function of the material considered of size i

$w_i(t)$ is the mass fraction of size i present in the mill at time t

$b_{i,j}$ is the mass fraction arriving in size interval i from breakage of size interval j.

From then on, the particle size distribution of the material being milled can be predicted at any time along the process using Equation (2.6).

2.4 Effect of ball size

Experience shows that small balls are effective for grinding fine particles in the load, whereas large balls are required to deal with large particles. In addition, harder ores and coarser feeds require high impact energy and large media. And on the other hand, very fine grind sizes require substantial media surface area and small media (Napier-Munn *et al.*, 1996).

Finding the right size of balls for a specific feed material to ensure grinding efficiency has always been a challenge. An empirical rule which has been used for many years shows that there is a relationship between the size x of the particle to be ground and the ball diameter d. It is given by $x_m=K.d^2$ where K is the maximum breakage rate factor. On the one hand, Austin *et al.* (1976) reported that K is a constant of which value range from 10^{-3} to 0.7×10^{-3} for soft to hard materials; and on the other hand, Napier-Munn *et al.* (1996) found K to be in the order of 0.44×10^{-3}.

In this section the different equations used to address this question are revised. Empirical approaches are here based on experiments whereas theoretical ones are based on analytical descriptions of the process.

2.4.1 Empirical approaches

The selection function can be expressed by the following general equation

$$S_i = a(d).x_i^{\alpha}.Q(x_i) \tag{2.7}$$

where x_i is the size of the particle

d is the diameter of the media used for the test

$Q(x_i)$ is a correction factor

Austin and Brame (1983) demonstrated that the correction factor $Q(x_i)$ could be replaced by

$$Q(x_i) = \frac{1}{1 + (x_i/\mu)^{\Lambda}} \tag{2.8}$$

In Equation (2.8), μ is a function of ball diameter. It gives an indication on the effective size of breakage for a given ball diameter. The equation relating the value of the size x_m at which the rate of breakage is a maximum for a given material to the parameter μ is as follows:

$$\mu = x_m . \left(\frac{\Lambda}{\alpha} - 1 \right)^{1/\Lambda} \text{, on condition that } \Lambda > \alpha \tag{2.9}$$

As far as the effect of ball diameter on the breakage rate is concerned, two important correlations have been proposed. Using results of Kelsall *et al.* (1967/68), Austin *et al.* (1984) suggested two equations expressing the dependency of the breakage rate on the ball diameter. The set of equations is given below:

$$a = a_0 \left(\frac{d_0}{d} \right)^{\xi} \tag{2.10}$$

$$\mu = \mu_0 \left(\frac{d}{d_0} \right)^{\eta} \tag{2.11}$$

where a_0 and μ_0 are the reference breakage parameters corresponding to the ball diameter d_0

a and μ are the predicted breakage parameters for ball diameter d.

The combination of Equation (2.7), (2.8), (2.10), and (2.11) allows one to describe or predict the effect of ball size on the selection function. An example of predictions is shown in Figure 2.5.

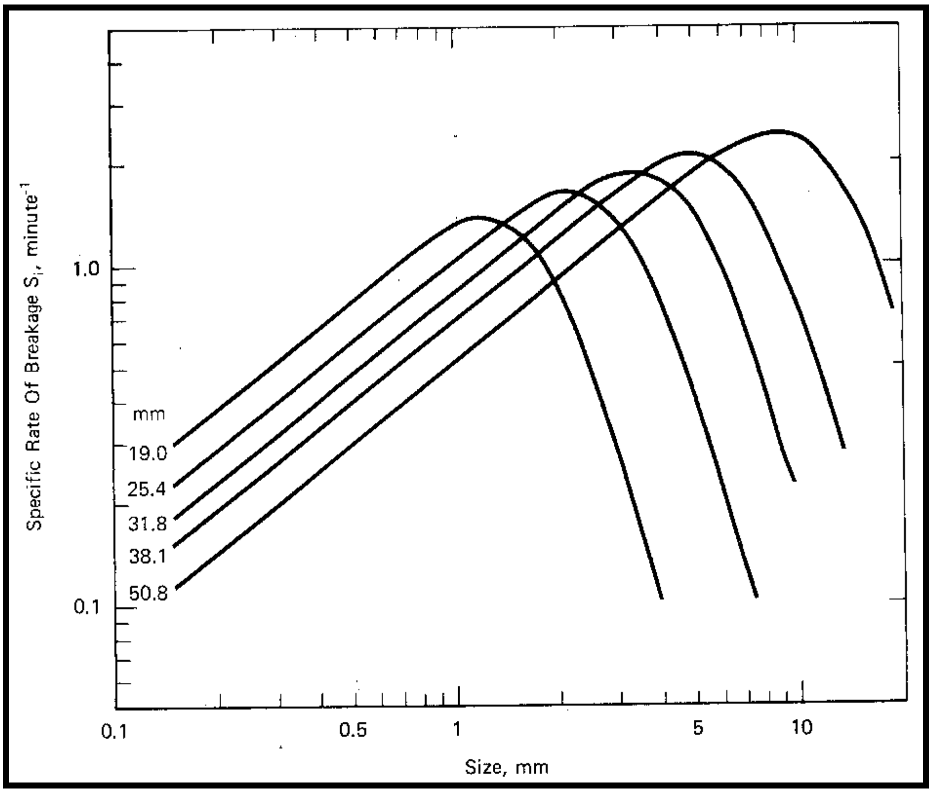

Figure 2.5 Predicted variation of S_i values with ball diameter for dry grinding of quartz (Austin *et al.*, 1984)

Later, Gupta *et al.* (1985) attempted to treat separately the effect of ball and mill diameters on the selection function. They reported to have got in nearly 90% of cases a deviation of about 1% in the predictions. Their general correlation for describing the effect of ball and mill diameters on the grinding rate parameters in dry grinding operation is presented below:

$$S_i = \frac{A^o D^{\gamma_G}}{\left(d - d^o\right)^{\beta_G}} x_i^{\alpha} \qquad (2.12)$$

In Equation (2.12) five material-dependent constants appear: α, β_G, γ_G, d^o, and A^o. Typical values found for γ_G approximately range from 0.25 to 0.61.

As for the ball size effect, they showed that it is reasonably given by:

$$a_1(d) = \frac{C'}{d^{\xi}} \tag{2.13}$$

where ξ is a parameter that has been shown to be independent on mill diameter for the same combination of media sizes

C' is a proportionality constant.

Another equation that is worth mentioning is the equation of Snow. Austin *et al.* (1976) reported the following expression:

$$\frac{S_i}{S_m} = \left(\frac{x_i}{x_m}\right)^{\alpha} \exp\left(-\frac{x_i}{x_m}\right) \tag{2.14}$$

where x_m is the feed size at which S_i is the maximum value S_m.

Some researchers claim that this type of equation is not suitable for describing the selection function (Austin *et al.*, 1976; Kotake *et al.*, 2002). It seems to them that Equation (2.14) cannot sufficiently explained the dependency of the dimensionless grinding rate constant S_i/S_m on the feed size x_i. On top of that, a careful look at it reveals the equation to be invalid. Simply put, for x_i equal to x_m, S_i should be equal to S_m, which is not the case. For this reason, Kotake *et al.* (2004) revised Snow's equation and proposed the following:

$$\frac{S_i}{S_m} = \left(\frac{x_i}{x_m}\right)^{\alpha} .\exp\left(-c\,\frac{x_i - x_m}{x_m}\right) \tag{2.15}$$

where α and c are constants deduced from experimental data.

Perhaps, the most important point is that Equations (2.14) and (2.15) bring up the notion of normalized or reduced S_i and x_i values. The dimensionless breakage rate and feed size are defined as S_i/S_m and x_i/x_m respectively. It allows one to reduce all the selection curves corresponding to different ball diameters into one single curve with normalized feed size and grinding rate respectively on the x- and y-axes. As for the effect of ball size, the following relationships are used for Snow's equation (Kotake *et al.*, 2004):

$$x_m = A.d^B \tag{2.16}$$

$$S_m = A'.d^{B'} \tag{2.17}$$

where A, B, A', and B' are material-dependent constants.

2.4.2 Probabilistic approaches

Mill load behaviour has a profound impact on the efficiency of grinding. A better understanding of the load mechanics inside the mill would help to obtain valuable information on grinding. Unfortunately, balls are extremely difficult to track individually because of the randomness of their motions. For that reason, zones of breakage can be defined based upon the grinding mechanisms that occur inside the mill. As far as ball mills are concerned three major zones are generally considered: the grinding zone, the cascading zone, and the cataracting zone.

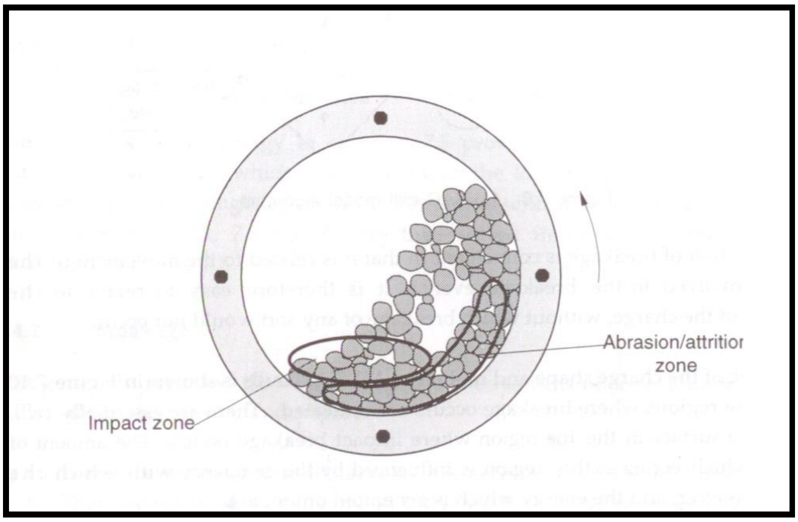

Figure 2.6 Breakage zones identified in a ball load profile (Napier-Munn *et al.*, 1996)

Figure 2.6 shows the two zones of breakage, i.e. the grinding zone in which impacts occur, and the abrasion zone. In the cataracting zone, particles are in free-flight motion and consequently no breakage occurs.

The theory of probability helps to get much insight on the general behaviour of the load. Most of the breakage takes place in the grinding zone in which balls in free-fall motion impact the material. The cascading zone is more prone to abrasion. In the cataracting zone, particles and media are in flight motion; as a result, nothing much happens in terms of breakage.

Nomura *et al.* (1991) tried to model breakage using the notion of breakage zones. Although various mechanisms of size reduction occur in the mill, impact breakage has been considered to be dominant in milling by balls. Basically, for breakage by impact to take place, a particle is to be nipped, or caught between two colliding balls, then crushed with sufficient collision energy. To describe this, two probabilities were introduced: the probability of nipping a particle in a single collision, and the probability of crushing a nipped particle by collision.

Nomura *et al.* (1991) then defined the specific rate of breakage or selection function as the fracture probability of a particle. The probabilistic definition of the selection function is given below:

$$S(x) = \frac{Z_{ef} V_G P_n(x) P_c(x)}{f_c V_M} \tag{2.18}$$

where Z_{ef} is the frequency of collisions effective for crushing

V_G is the volume of the zone of possible nipping in the grinding zone

$P_n(x)$ is the probability of nipping a particle of size x by two approaching balls

$P_c(x)$ is the probability of crushing a particle of size x nipped by two colliding balls

f_c is the fraction of mill volume occupied by the bulk volume of powder charged

V_M is the mill volume.

Using appropriate simplistic assumptions, Kotake *et al.* (2004) derived the following theoretical equation:

$$S_i = C_1 d^m x_i^\alpha \exp\left(-C_2 \frac{x_i}{d^{n_0}}\right) \tag{2.19}$$

where C_1, C_2, m and n_0 are constants.

Letting m=0.25 and n_0=1 Equation (2.19) reduces to:

$$S_i = C_1' d^{0.25} x_i \exp\left(-C_2' \frac{x_i}{d}\right) \quad (2.20)$$

derived by Tanaka and in which C_1' and C_2' are constants.

The key point in Tanaka's equation is that it can be utilized to investigate the change of the grinding rate constant as a function of ball diameter and feed size.

As for Nomura *et al.* (1991), the theoretical selection function was derived as follows

$$S(x) = \left[\frac{Z_{ef} C_1}{f_c V_M \lambda}\right] x^{(5b/3)+1} \left[\frac{q(x)\{1-(x/\lambda)\}^2}{\{1+(x/d_b)\}^{1/3}}\right] \quad (2.21)$$

where Z_{ef} is the frequency of collisions effective for crushing

λ is the average ball-ball distance in the grinding zone. It has been shown to vary with mill operating conditions

C_1 is given by $C_1 = \left[\frac{\pi \beta_N \eta_N}{6A_r(1-\varepsilon_p)}\right](2M_b V_r^2)$ with A_r is a constant showing the material strength, and β_N and η_N are constants independent of material and operational conditions. M_b is the mass of a ball whereas V_r is the mean relative velocity of ball. And ε_p represents the void fraction of a static bed.

$q(x)$ is a function of the probability of crushing of a nipped particle.

Substituting the following $a=Z_{ef}C_1/(f_c.V_M.\ \lambda)$ and $\alpha=(5b/3)+1$ into Equation (2.21) allows to get back to Equation (2.7), but this time with the corresponding correction factor given by

$$Q(x) = \frac{q(x)\{1-(x/\lambda)\}^2}{\{1+(x/d_b)\}^{1/3}}$$

where α, defined as a distribution parameter, now proven theoretically to be material characteristic as usually assumed in empirical models.

However, for practical milling, *q(x)* and the denominator of *Q(x)* have been found to be close to unity, leading to the following expression

$$Q(x) \approx [1-(x/\lambda)]^2 \tag{2.22}$$

Finally, the effects of the ball diameter and density on a are experimentally (Nomura *et al.*, 1991) found to be related as follows: $a \propto \rho_b / d$.

2.5 Abnormal breakage

Abnormal breakage in laboratory mills may be defined as departure from first-order kinetics, and occurs particularly for the larger particle sizes in the mill feed (Austin *et al.*, 1973). Later on, Austin *et al.* (1977) studied the abnormal breakage and proposed several models that may explain it. First, they assumed the material to consist of an initial material A that breaks to produce another material B. The two materials are different only on a breakage point of view. Then, during grinding, component A is breaking to component B. In doing so, they found the following model:

$$w_i(t) = \frac{m(t)}{m(0)} = (1-\phi_i)e^{-S_A t} + \phi_i . e^{-S_B t} \tag{2.23}$$

where $\phi_i = \dfrac{b'_{ii} S_A}{S_A - S_B}$

S_A is the selection of component A of the material

S_B is the selection function of component B of the material.

In overall, the system behaves as if the A material consists of a fraction 1-ϕ_i of soft material and a fraction ϕ_i of harder material.

In general the effective mean value of the selection function is given by

$$S_i = \frac{1}{\dfrac{1}{S_{Ai}} + \dfrac{b'_{ii}}{S_{Bi}}} \tag{2.24}$$

Because not all the non-first-order grinding batch grinding can be fitted with Equation (2.23), a more elaborated has been proposed. Second, they assumed the feed A breaking to an intermediate material B which in turn breaks to a final material C. The corresponding model is as follows:

$$w_i(t)=\frac{m_i(t)}{m_i(0)}=\left\{1+S_A t+\left(\frac{S_A}{S_A-S_C}\right)^2\left[(S_C-S_A)t-1\right]\right\}.e^{-S_A t}+\left(\frac{S_A}{S_A-S_C}\right)^2 e^{-S_C t} \qquad (2.25)$$

Here the effective mean value of the milling rate is approximately given by

$$S_i=\frac{1}{\frac{1}{S_{Ai}}+\frac{1}{S_{Bi}}+\frac{1}{S_{Ci}}} \qquad (2.26)$$

In conclusion, for larger sizes, it is found that the disappearance of material from a given top size interval is often not first order, but can be modelled as consisting of a faster initial rate and a slower following rate. We refer to the first-order breakage of smaller sizes as normal breakage and to the non-first-order breakage of larger sizes as the abnormal breakage region. When a particle size exhibits an abnormal behaviour, Austin *et al.* (1984) suggests the mean effective specific rate to be defined by the time required to break 95% of the material. Alternatively Equation (2.24) can be used.

2.6 Effect of ball mixture

2.6.1 Ball size distribution in tumbling ball mills

During the grinding operation, the object is to hold an equilibrium charge where the rate of addition of the number and mass of balls equals the rate at which the number of balls are eroded and expelled from the mill plus the rate of loss in mass of balls due to abrasion and wear. That is, the grinding conditions remain constant. The initial charge should be as identical as possible to the equilibrium charge.

The ball charge in a mill is never constituted of uniform sizes of balls; it is rather a mixture of balls of different sizes ranging from small up to bigger balls that are newly added.

One of the most difficult questions to address and indeed the most important to answer in the optimal design of ball milling circuits is the choice of the mixture of ball sizes to be used in the mills. Plants have generally developed in-house solutions to this problem.

The equilibrium ball size distribution is a function of the makeup policy and the wear mechanism. Menacho and Concha (1986) have addressed this issue. They considered the general model of ball wear in a mill proposed by Austin and Klimpel (1986):

$$\frac{dM_b(t)}{dt} = -k.r_b^{2+\Delta} \tag{2.27}$$

where $M_b(t)$ is the ball mass after time t

r_b is the ball radius

k is a constant whose dimensions depend on the value of Δ

Δ is a constant defining the ball wear law.

In the differential equation (2.27), it is assumed that the mass wear rate of a piece of spherical media (mass per unit time) is a power function of its radius r. Thus if Δ=0, the wear rate is proportional to the surface area of the ball. It is called the Bond wear law or the surface law. On the contrary, if Δ=1, the ball wear follows the Davis wear law or the mass wear law.

Experimental data have reported a Δ-value of 2 can also be obtained especially for wet milling (Austin and Klimpel, 1985).

Using a phenomenological approach, Menacho and Concha (1986) have derived the solution of Equation (2.27). Their solution represents in fact a general model for the dynamic ball size distribution in a ball mill.

With appropriate assumptions, the steady-state ball size distribution can be deduced. And if the wear law is given (Δ is given), the general steady-state ball size distribution model is expressed as follows:

$$M_3^{ss}(d) = \frac{\left[d^{4-\Delta} - d_0^{4-\Delta}\right] + \sum_{k=1}^{p} m_0^{\mathrm{I}}(d_k)\left\{d_k^{4-\Delta} - d^{4-\Delta}\right\}U(d - d_k)}{\sum_{k=1}^{p} m_0^{\mathrm{I}}(d_k)\left\{d_k^{4-\Delta} - d^{4-\Delta}\right\}} \tag{2.28}$$

where M_3^{ss} is the cumulative mass distribution of balls at steady-state

d_k is the diameter of balls in the makeup

d is the diameter of balls in the charge

Δ is the wear rate factor

m_0^{I} is the relative number frequency of balls in the makeup

p is the number of ball classes in the makeup

U is the unit step function defined as follows $U(d) = \begin{cases} 0 & \text{for } d < 0 \\ 1 & \text{for } d \geq 0 \end{cases}$

For respectively one and two ball sizes in the makeup, Equation (2.28) can be reduced to the equilibrium ball size distribution proposed by Austin and Klimpel (1985):

$$M(d) = \frac{d^{4-\Delta} - d_{\min}^{4-\Delta}}{d_{\max}^{4-\Delta} - d_{\min}^{4-\Delta}}, \text{ for one ball size} \tag{2.28}$$

$$M(d) = \begin{cases} \dfrac{d^{4-\Delta} - d_{\min}^{4-\Delta}}{K_1 d_1^{4-\Delta} + (1-K_1) d_{\min}^{4-\Delta}} & \text{for } d_{\min} \leq d \leq d_2 \\ \dfrac{K_1 d^{4-\Delta} + (1-K_1) d_2^{4-\Delta} - d_{\min}^{4-\Delta}}{K_1 d_1^{4-\Delta} + (1-K_1) d_2^{4-\Delta} - d_{\min}^{4-\Delta}} & \text{for } d_2 \leq d \leq d_1 \end{cases}, \text{ for two ball sizes} \tag{2.30}$$

where $K_1 = \left[1 + \left(\frac{m_2}{m_1}\right)\left(\frac{d_1}{d_2}\right)^3\right]^{-1}$ and thus lies between 0 and 1.

For a single ball size d in the makeup Equation (2.29) applies, whereas Equation (2.30) is used for a makeup of balls consisting of two ball sizes d_1 (d_1=$d_{\max}$) and d_2 for which mass fractions are m_1 and m_2 respectively.

If the ball wear follows the Bond law, that is Δ=0, it is possible to show that the fraction number of media in the mill at steady-state is related to the diameter of the balls as follows (Yildirim and Austin, 1998):

$$\frac{d}{d_{\max}} = 1 - \left(\frac{2k_1\tau}{d_{\max}}\right).\overline{N}(d) \tag{2.31}$$

where $\overline{N}(d)$ is the fraction by number of media with radii greater than d

$d_{\min} = d_{\max} - 2k_1\tau$ is the diameter of the ball leaving the mill after being worn down

k_1 is a constant which represents rate of change of radius in Bond wear law

τ is the maximum life of the media in the mill due to wear.

Equation (2.31) shows that the equilibrium charge consists of equal number of balls in each ball class providing the class widths are the same. In other words, according to Bond law, the equilibrium ball charge distribution is in statistical terms a constant number distribution function.

2.6.2 Milling performance of a ball size distribution

The overall effect of a mixture in the mill may be taken as the linear weighted sum (Austin *et al.*, 1984),

$$\overline{S_i} = \sum_{k=1}^{m} m_k S_i(d_k) = \sum_{k=1}^{m} m_k S_{i,k} \tag{2.32}$$

where m_k is the relative mass frequency function of balls of size d_k.

$S_i(d_k)$ is the selection function of particle size x_i due to balls of size d_k

Let $b_{i,j,k}$ be the fractional breakage into size i from breakage of size j by size k balls. The mean breakage function is given by the ratio between the total specific rate of breakage into size i and the total specific rate of breakage from size j, that is,

$$\overline{b}_{i,j} = \sum_{k=1}^{m} b_{i,j,k} S_{i,k} m_k \Bigg/ \sum_{k=1}^{m} S_{j,k} m_k \tag{2.33}$$

If $b_{i,j,k}$ is not a function of k, Equation (2.33) reduces to $\overline{b}_{i,j} = b_{i,j}$.

We will assume this to be true, that is, one set of $b_{i,j}$ values only will be used. We will further assume, on the basis of rather limited experimental information, that $b_{i,j}$ values do not change with mill conditions or mill diameter in the region of usual operating conditions. Figure 2.7 gives an illustration of a material of quartz that has been milled under various conditions. Despite the change in milling conditions, the quartz material has presented a normalizable behaviour for the breakage function.

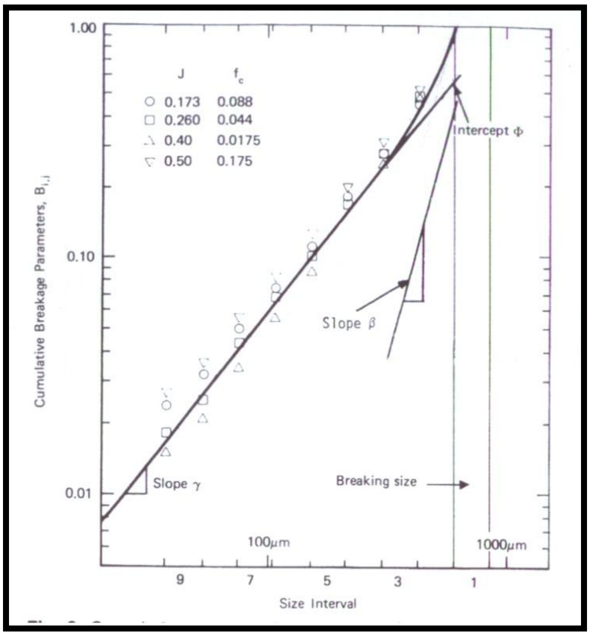

Figure 2.7 Breakage function of a 850×650 microns normalizable quartz under various mill load conditions (D=195 mm, d=25.4 mm, ϕ_c=0.7) after Austin *et al.* (1984)

2.7 Summary

The review of the literature has revealed several key points that are listed below.

The widely accepted empirical form for the selection function model is given by:

$$S_i = a.x_i^{\alpha}.Q(x)$$

where a is the grinding rate constant and α is the distribution parameter of the material.

$Q(x)$ is a correction function varying from 1 to 0 with increasing x but is rather insensitive for relatively small x. The most important expressions factors that have been reported so far for the correction factor $Q(x)$ are the following:

1° $Q(x) = \exp(-k.x)$ (Austin *et al.*, 1976; Kotake *et al.*, 2004; Snow's equation; Tanaka's equation)

2° $Q(x) = G\left[\frac{\ln(x/\mu)}{\ln\sigma}\right]$ where $G(x) = \frac{1}{\sqrt{2\pi}}\int_{-\infty}^{x} e^{u^2/2}.du$ is the Gaussian or normal distribution function (Austin *et al.*, 1976)

3° $Q(x) = \frac{1}{1+\left(\frac{x}{\mu}\right)^{\Lambda}}$ (Austin *et al.*, 1984)

The breakage function is generally regarded as normalizable for most of the materials found.

The effect of ball size gives rise to several questions pertaining to η and ξ. Various values of η have been reported in the range 1 to 2, whilst ξ has been about 1 (Kelsall *et al.*, 1967; Austin *et al.*, 1976; Austin *et al.*, 1984; Yildirim *et al.*, 1999; Kotake *et al.*, 2004; Austin *et al.*, 2006). Only a detail investigation on a South African coal will allow to establish with confidence the values to use for our particular cases.

Considering the availability of the documentation at hand, the effect of ball size distribution is accepted to be the weighed sum of the individual contribution of balls to grinding.

In their conclusion, Concha *et al.* (1992) quoted the following: “Further progress will require refinement of the mill simulator model, in particular more detailed investigations of the effect of ball diameter on breakage rates, primary fragment distributions and mill performance.” As a consequence of this statement, it is believed that an investigation of the effect of ball size and ball size distribution on a South African coal is worth the effort.

Chapter 3 Experimental equipment and programme

The Mineral Processing Research Group of the Centre of Material and Process Synthesis (COMPS) initiated in October 2007 an industrial survey. The main objective was to collect enough feed coal for this project from Tutuka Power Station in South Africa. Media and mill feed coal had to be sampled for laboratory purposes. A total coal mass sample of 250 kg was collected from a selected mill feed. And 150 kg of grinding media was carefully prepared from a regraded mill load. Three ball sizes were considered: 30.6 mm, 38.8 mm, and 49.2 mm; and in each case, 50 kg of media was constituted.

Using the Wits pilot mill, a series of batch tests had to be carried out under different mill conditions. To fully characterize the breakage properties of this coal, three ball sizes and two ball mixtures were used.

In this chapter, the experimental equipment and programme in the laboratory are presented: how batch tests were done, particle size analysis, feed preparation, and ball size preparation.

3.1 Laboratory grinding mill configuration

Wits laboratory mill was used to carry out the necessary batch grinding tests on the coal sample from the plant. This mill is fitted with twelve equally spaced trapezoidal lifters and is driven by a 2.5 kW variable speed motor mounted on a mill rig. The internal dimensions of the mill are 0.54 m diameter and 0.20 m length. The lifters are 20 mm high with 45 degrees face angle and 50 mm base width.

Table 3.1 gives some specifications about the mill and the operating conditions as defined for the experimental work. A photograph of the laboratory mill is also presented in Figure 3.1. For a full description of the mill, readers are referred to more detailed papers on the matter (Liddell and Moys, 1988; Moys *et al.*, 1996).

Table 3.1 Laboratory operating conditions

Mill dimensions	*Diameter* *Length* *Volume*	*540 mm (inside liners)* *200mm* *0.0444 m^3*
Liner configuration	*Number* *Shape*	*12* *Trapezoidal* *20 mm height* *50 mm base width* *45 degrees face angle*
Test conditions	*Ball filling, J* *Powder filling, U* *Mill speed*	*20 %* *75 %* *75 % of critical speed*

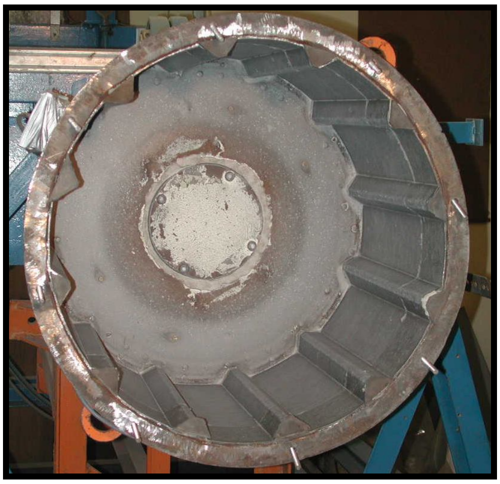

Figure 3.1 Snapshot of the laboratory mill

3.2 Preparation of mono-size grinding media

In order to carry out the necessary laboratory tests, three different ball classes as narrow as possible needed to be prepared. First, media were collected at Tutuka Power Station. Then, balls were individually weighed and their mass recorded. After data analysis, balls within predefined mass intervals were selected to constitute the population of interest. With the ball density (7.62 g/cm^3) and the mass ranges defined, ball sizes could finally be calculated. Specifically, three sizes were retained: 30.6 mm, 38.8 mm, and 49.2 mm.

As far as the ball mixtures are concerned, two mixes were considered:

1° The first mixture was constituted of the same number of balls the six ball size intervals considered. And for the purpose of comparison, this charge has been called "Equilibrium Ball Size Distribution" EQM-BSD.

2° The second mixture, on the other hand, is constituted of the same mass of balls in the six ball classes. It is here referred to as "Original Equipment Manufacturer recommended Ball Size Distribution" OEM-BSD.

Equal numbers of balls in each size class results when the ball wear rate is constant and a fixed top size of ball is fed to the mill. OEM-BSD on the contrary is recommended by the OEM at Tutuka Power Station. It implies more balls of small sizes, and consequently, an increase in the total surface area and an increase in the rate of milling of fine particles.

Table 3.2 presents the two ball size distributions as considered for the tests. In each case the mass of the load was calculated to be 41.2 kg for an average bed porosity of 0.4 (Austin *et al.*, 1984).

Table 3.2 Ball mixtures used for experiment.

	EQM-BSD		OEM-BSD	
Ball classes (mm)	*Mass fraction (%)*	*Ball number*	*Mass fraction (%)*	*Ball number*
50.0 – 44.0	*40.0*	*40*	*16.6*	*17*
44.0 – 37.5	*25.8*	*40*	*16.7*	*27*
37.5 – 31.5	*15.8*	*38*	*16.6*	*37*
31.5 – 26.5	*9.3*	*38*	*16.7*	*70*
26.5 – 22.4	*5.6*	*40*	*16.7*	*126*
22.4 – 19.0	*3.4*	*40*	*16.7*	*224*

3.3 Feed material preparation

3.3.1 Coal sample collection at Tutuka power station

A large coal sample was obtained from a mill feed at Tutuka Power Station for laboratory tests. From the inlet of the mill, a sampling pipe was inserted into the feed stream to collect coal samples. Twelve plastic bags were filled with approximately 20 – 25 kg of coal each. Globally, 250 kg of coal was collected.

Internal references reported the average coal particle density as established in routine inspection at Tutuka Power Station to be 1.57 g/cm^3. The humidity of the coal was found after preliminary laboratory tests to be approximately 5.23 %.

3.3.2 Feed preparation for laboratory tests

With the test conditions defined in Table 3.1 the necessary mass of material (powder) per test to be used was calculated to be 2.507 kg for a specific density of 1.57 g/cm^3. Knowing this, a total of 26 mono-sized feed materials was prepared for the intended series of grinding tests (Table 3.3).

The coal collected at the plant was first to be roughly sorted by particle size classes. To do this, batches of approximately 2 kg of coal were one after another screened for about 5 min. Fractions of coal retained on the screens of interest as depicted in Table 3.3 were accumulated in labelled plastic bags. After that, a further screening of 20 min on the sorted mono-sized coal in each plastic bag was done to get a bulk mono-sized mass more carefully prepared. Finally, the different masses obtained which were ready for batch testing were split using a Jones riffler to constitute 2.507 kg representative feed coal samples. After this last step in the preparation, feed samples were ready for batch test.

To sum up: on the one hand, eight single sized feed coal samples were prepared for the EQM-BSD tests. And on the other hand, seven samples were considered for the OEM-BSD. As for the single ball sizes 4, 4, and 3 feed sizes were constituted respectively for tests using 49.2, 38.8, and 30.6 mm balls. Table 3.3 gives a summary of the sizes that were milled in each case.

__Table 3.3 Experimental design__

Feed size (microns)		Ball charge considered				
Upper	Lower	EQM-BSD	OEM-BSD	30.6 mm	38.8 mm	49.2 mm
26 500	22 400	×	×		×	
22 400	19 000					×
19 000	16 000	×	×			
16 000	13 200			×	×	
13 200	9 500	×	×			
9 500	6 700			×		×
6 700	4 750	×	×		×	
4 750	3 350					
3 350	2 360	×	×			
2 360	1 700			×	×	×
1 700	1 180	×	×			
1 180	850					
850	600	×				
600	425		×			
425	300					×
300	212	×				

3.4 Experimental procedures

3.4.1 Experiment design

The programme presented in Table 3.3 was designed and followed to achieve the objective of the present study.

Tests on single ball sizes were used to determine the breakage characteristics of coal. Table 3.4 presents the single sizes considered, their respective number for a total mass of 41.205 kg in the mill load.

__Table 3.4 Mono-sized media charges used__

Ball size [mm]	30.6	38.8	49.2
Ball number	358	181	89
Total mass [kg]	41.205	41.205	41.205

To illustrate how Table 3.3 is to be used, one would infer that particles in the size interval 9500 – 6700 microns was batch milled using 38.8 mm ball media. Another example would be the size interval 300 – 212 microns and the EQM-BSD.

Mono-sized media charges presented in Table 3.4 will be used for characterizing the breakage properties of the coal under study. Tests on the EQM-BSD are for investigating the effect of ball size distribution on milling rate whereas those on the OEM-BSD serve for validation.

3.4.2 Batch grinding tests

Broadly speaking, batch grinding tests are performed using the procedure known as the one-size-fraction method (Austin *et al.*, 1984).

In our experimental work, three grinding times were considered: 0 – 0.5; 0.5 – 1; 1 – 2 min. For every test, a blank sieving test was done on the prepared feed material. After that, the coal sample was placed in the mill with the media of appropriate size. The feed size and media size were mixed in accordance to the programme in Table 3.3. Next, the feed material was ground for 30 seconds; then, analyzed. The mill was emptied after this time period through a grate to retain the grinding balls. A full particle size distribution was done on the collected product from the top screen down to the 75 microns screen.

First, the product was screened down to 1700 microns. Then, the undersize material (i.e. -1700 microns) was split to constitute a 100 g representative sample. Second, the 100 g sample was wet washed on a 75 microns screen to remove the dust. Then, a drying in the oven at 50°C followed. Finally the dried coal was screened to complete the size analysis. For materials of size below 1700 microns, a 100 g sample was directed prepared for wet screening, then dry screening after the washed sample was dried in the oven.

After all this, the material was then recombined for batch grinding for an extra 30 seconds, followed by size analysis. The process was finally repeated for 60 more seconds. As for materials of size less than 1700 microns, coal samples were milled for a total time of 4 min, i.e. a fourth time period 2 – 4 min was added for the full test.

3.4.3 Particle size analysis

Dry sieving was always performed for about 20 minutes. The complete size analysis was made using a stack of sieves, starting with the top size of the feed size interval all the way done to 75 microns.

For materials coarser than 1700 microns, size analysis was performed in two steps. First, a dry screening of the material was done for 20 minutes down to 1700 microns. Then, the material in the pan (-1700 microns) was split to obtain a 100 g mass sample. The small sample was wet washed on a 75 microns screen to remove the fines (-75 microns). Then, the washed sample was dried in the oven at 50°C. The dried sample was weighed, and then screened for 20 minutes using nested screens from 1700 down to 75 microns.

For materials smaller than 1700 microns, size analysis was done in a single step. The material was split to get a representative sample of about 100 g. Then, this was followed by the wet screening on a 75 microns screen. During wet screening, the fines were removed. The wet material retained on the 75 microns screen was dried until water was left out. Then a dry screening was done for 20 minutes.

In either case, the mass fraction retained on each screen was weighted on a scale. The same screens were used throughout the experiments to keep the consistency. The dried weight of the washed sample was checked against the starting mass sample before wet screening. The difference in mass was then added to the mass in the pan to ensure that masses balance out.

3.5 Data collection and processing

As soon as the raw data were recorded on a paper worksheet, an electronic spreadsheet package was used to compile the information. Then a spreadsheet programme was developed to generate different particle size distributions. The necessary information on the process was produced for further analysis. Using Equations (2.2), (2.10) and (2.11) and manipulated raw data, the different grinding parameters could be estimated. This detailed analysis aimed at bringing light on the behaviour of the coal used at Tutuka Power Station.

A computer was utilized to constitute a database. In other words, all data obtained from each experiment was stored in the computer and the required output printed out. Relevant results of the manipulated raw data were produced and stored in the same way. After the breakage parameters were estimated, the selection functions of the two ball mixes were predicted and compared to the results found with EQM- and OEM-BSD's.

The next two chapters of this dissertation explain in much detail the parameter estimation side of the work and the significance of the results obtained.

3.6 Summary

The disappearance rate of feed size material was monitored for three grinding times; namely, 0 – 0.5; 0.5 – 1; and 1 – 2 minutes. A fourth grinding time was added for particle sizes less than 1700 microns. Grinding times were recorded at each step for future data processing. The material ground was then taken out of the mill after the set grinding time and a complete particle size analysis was done. The compiled raw data was stored on a computer. This had then to be manipulated and integrated in an analysis in order to produce valuable information leading to the characterization of Tutuka coal.

Chapter 4 Characterization of coal breakage properties

Austin *et al.* (1984) have shown that the breakage characteristics of any materials could be determined using single-size-fraction batch grinding tests. Generally, mono-size balls are used to batch-grind single size materials for several time periods in order to have an estimate of the grinding kinetics.

In this chapter, raw data collected from laboratory batch tests performed using three different media sizes, namely 30.6, 38.8, and 49.2 mm are processed to provide different breakage parameters necessary to describe the selection and breakage functions of the coal from Tutuka Power Station. Ultimately, parameters α, μ, η, and ξ are determined for the selection function; and parameters β, γ, and Φ for the breakage function.

4.1 Introduction

For many years, the breakage parameters have been estimated using graphical methods. Such techniques are less accurate, biased and time consuming. Furthermore, an appropriate scale and spacing between tick marks are supposed to be chosen carefully to reasonably measure some parameters off the plotted graph. That is why, in this chapter all the breakage parameters are determined numerically starting with the milling rate values themselves up to the breakage parameters. This set of information is then interpreted in connection with milling in general.

The most important note to make is that the characterization of the breakage properties of any material is generally done using data relative to single ball size tests. In our case, the particle size distributions derived from the size analysis on the three ball sizes are used for this purpose.

4.2 Determination of selection function values

4.2.1 Non-linear regression technique

The experimental size distributions of the different mill products at times 0 – 0.5 – 1 – 2 – 4 min were used to get an estimate of the selection function. A non-linear regression technique was implemented on the data. Basically, this technique aims at finding the best combination of fitting parameters of a model by minimizing the square of the differences between the experimental values $P_{expt}(t)$ and the predicted ones $P_{model}(t)$. And here the model referred to is the first order breakage law. With this in mind, the objective function is ultimately defined as

$$SSE = \sum_{r=1}^{R} \left[P_{expt}(t) - P_{model}(t) \right]^2 \tag{4.1}$$

where R is the number of runs considered to carry out a full batch test on a given particle size x. If the full test is done for, say 0, 0.5, 1, and 2 min successively, R=4

$P_{expt}(t)$ retained experimental mass fraction on the top size screen x at grinding time t

$P_{model}(t)$ predicted mass fraction retained on size screen x_{i+1} after grinding of single-sized coal material of initial size x_i for a total grinding time t.

A good example of this is plotted in Figure 4.1 where the retained mass fraction is plotted against grinding time on a log-linear scale. In this case, data relative to a mono-sized coal material (-2360 +1700 microns) for the three media sizes are compared. It is observed that the results follow the first order grinding hypothesis. Similar graphs can be produced for the other particle sizes using the data in Tables A.1 to A.26 in Appendix A.

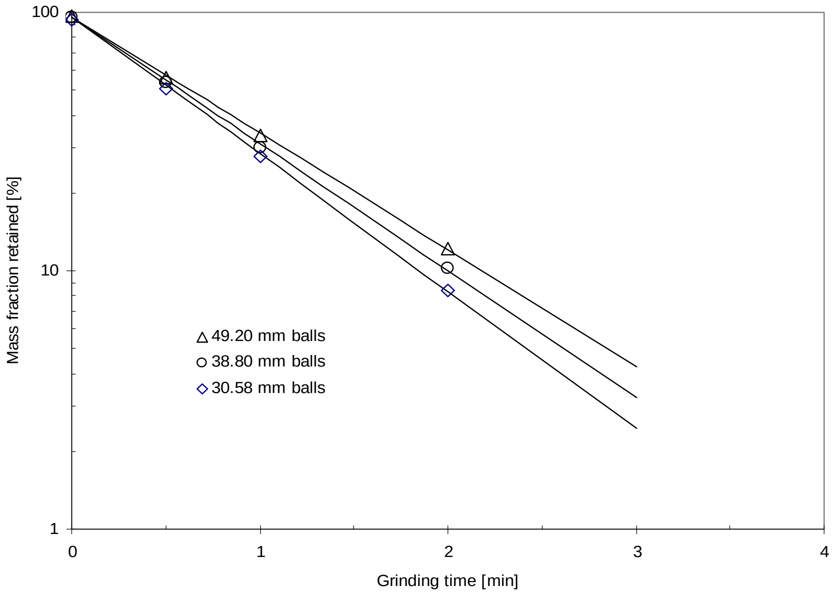

Figure 4.1 Selection functions as obtained for three media diameters grinding mono-sized coal materials. In this case (-2360 +1700 microns)

As for the abnormal breakage, the material was assumed to be constituted of two fractions: a fast-breaking fraction and a slow-breaking one (Austin *et al.*, 1977). Equation (2.23) was therefore considered for non-linear regression. For our particular case study, this equation can be rearranged as follows:

$$w_i(t) = \frac{m(t)}{m(0)} = (1-\phi_i)e^{-S_{fast}t} + \phi_i.e^{-S_{slow}t} \qquad (4.2)$$

where S_{slow} and S_{fast} are the grinding rates of the slow- and fast-breaking fractions constituting the material

ϕ_i represents the fraction of the slow-breaking fraction of the material.

In order to define the effective average selection function value, Austin *et al.* (1984) recommend first to get the time required to break 95 % of the material, then work out the grinding rate. In our case study, Equation (2.24) was used to model the abnormal behaviour. Once this was done, the time needed to get 5 % of the initial mass remaining on the top screen size was determined. Finally, this time was substituted in the first-order law solution to calculate the mean effective selection function.

4.2.2 Determination of selection function parameters

The same basic principle described in Section 4.2.1 above was applied for coal breakage characterization. Equation (2.2) was used to reduce the number of parameters to three, i.e. a, α and μ. Parameter Λ was fixed as 3 (Austin *et al.*, 1984) since our experiments did not provide sufficient information to allow accurate determination of Λ. Parameter α was assumed to be equal to a single value for all three ball size classes following Austin *et al.* (1984). The value of α that was found to satisfactorily characterize breakage rate is 0.81.

Values of a and μ for the three ball sizes are presented in Table 4.1.

As a starting point, different values of breakage rate as obtained from batch tests were compiled. Using again the same non-linear technique, the breakage parameters a and μ were searched for α=0.81 and Λ=3. Parameters providing best fits (Table 3) were then substituted in Equation (2.2) to plot Figure 4.2. This figure presents three graphs corresponding to ball sizes of 30.6 mm, 38.8 mm and 49.2 mm, using the same size interval of material, i.e. -2360 +1700 microns.

It can be seen from Table 4.1 that a-values decrease with increasing ball diameters and that μ-values increase and consistently shift towards coarser particle sizes for bigger balls. This observation confirms the expected behaviour (Austin *et al.*, 1976).

Table 4.1 Selection function parameters

Ball size (mm)	a	μ	α	Λ
30.6 ± 1.3	*0.62*	*11.5*	*0.81*	*3*
38.8 ± 0.6	*0.48*	*19.3*	*0.81*	*3*
49.2 ± 0.5	*0.39*	*31.1*	*0.81*	*3*

4.3 Effect of ball size

4.3.1 Breakage rate as a function of ball size

To study the effect of ball diameter on the selection function, Equations (2.10) and (2.11) are used. In these two equations, the factor ξ relates *a*-values to the ball size while the factor η does the same between μ-values and the ball size.

Considering the values in Table 4.1, a parameter search was implemented on ξ to define the relationship *a*-versus-*d*. The value found was 1.07 ± 0.1 which confirms the value of 1 proposed by Austin *et al.* (1984).

Similarly, the factor η was searched for. This time, η was found to be 2.08 ± 0.1.

The point to make here is that the value of η=2 has been proposed by Kelsall *et al.* (1967) and then confirmed by Austin *et al.* (1976), which implies a surface wear mechanism. Recently, many values have been reported and it is still unclear what might be the reason for these diverging findings (Yildirim *et al.*, 1999; Kotake *et al.*, 2004; Austin *et al.*, 2006).

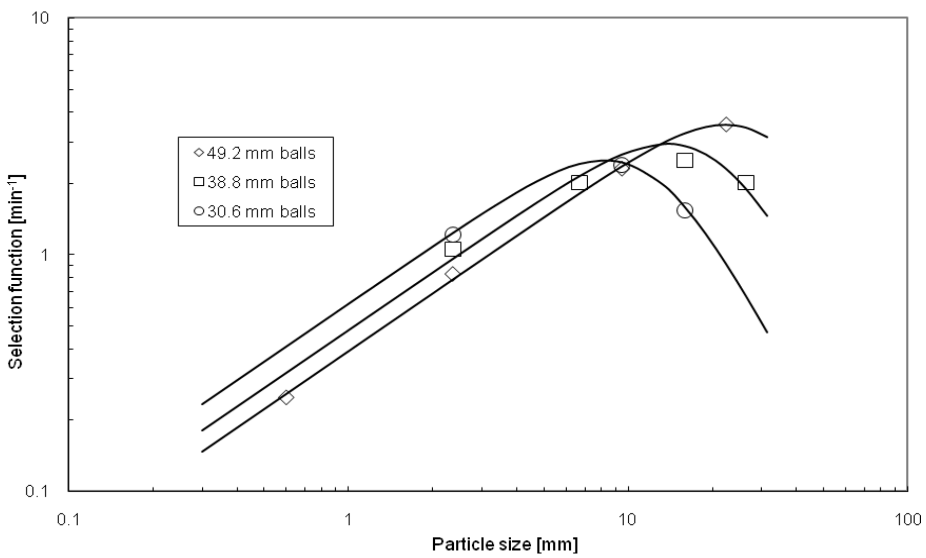

Figure 4.2 Effect of ball diameter on the selection function

With the two exponent factors (i.e. ξ and η) found, the effect of ball size on the selection function was completely characterized. This is depicted in Figure 4.2 for the three ball diameters used in the laboratory. Thus, the change in the selection function with particle size for any other ball size can be predicted for the coal.

4.3.2 Reduced selection function

In this section, an attempt to fit the data with Snow's equations is made to take advantage of the notion of reduced selection function. Equation (2.14) and (2.15) are used to evaluate its validity against laboratory results (Appendix C).

In the first attempt, Equation (2.14) was fitted to the dimensionless grinding rates results with α being 0.81. Figure 4.3 shows the findings. As it can be seen, the fit is quite far off the data points and as mentioned earlier in the literature review, this equation is not even valid. In the second attempt, Equation (2.15) was tested against the measured data. Here again, the fit is not more impressive than the previous even though this time it seems to be closer to the data points.

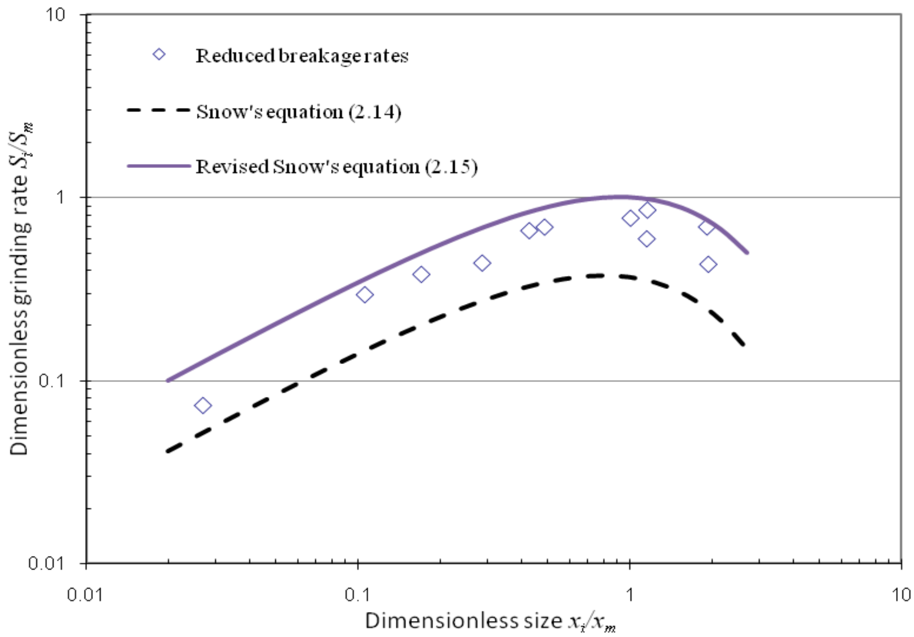

Figure 4.3 Reduced selection function graph

In conclusion, whether it is Snow's equation or the revised Snow's equation, none seems to work well for this coal. This implies that functions representing $Q(x)$ of the exponential form in Equation (2.7) are not good fits for our results. Though the data points seem to present a pattern, it is difficult to satisfactorily fit them with the available models. Consequently, there is little evidence that Equations (2.15), (2.19), and (2.20) are applicable in this case study.

4.4 Breakage distribution function

To estimate the cumulative primary breakage distribution values the single-size fraction B-II method was used. Austin *et al.* (1984) showed that B_{ij} values can be estimated from size analysis of the product from grinding of size j materials as:

$$B_{ij} = \frac{\log\left[\left(1-P_i(0)\right)/\left(1-P_i(t)\right)\right]}{\log\left[\left(1-P_{j+1}(0)\right)/\left(1-P_{j+1}(t)\right)\right]} \tag{4.3}$$

where $P_i(t)$ is the weight fraction of the material less than size x_i at time t.

They recommend in this method to use shorter grinding times that result in 20 – 30% broken materials out of the top size. These shorter times are meant to minimize re-breakage, and thereby get more accurate estimates of the breakage function parameters. However, a previous study (Austin and Luckie, 1971) showed that even at 65 % broken material the method is still accurate enough.

Taking into account the re-breakage limitation, only particle sizes with no more than 60% broken material on the top screen size at 0.5 min grinding time were considered for breakage parameter estimation. The B_{ij} values obtained using Equation (4.3) were then fitted to the empirical model given in Equation (2.5) and the breakage function parameters evaluated for the coal used.

Figure 4.4 illustrates how the cumulative primary breakage function curves has been fitted for the same particle size (-2360 +1700 microns) and the three single ball diameters. The average breakage parameters used for the fit were β = 3.2, γ = 0.53, and Φ = 0.51

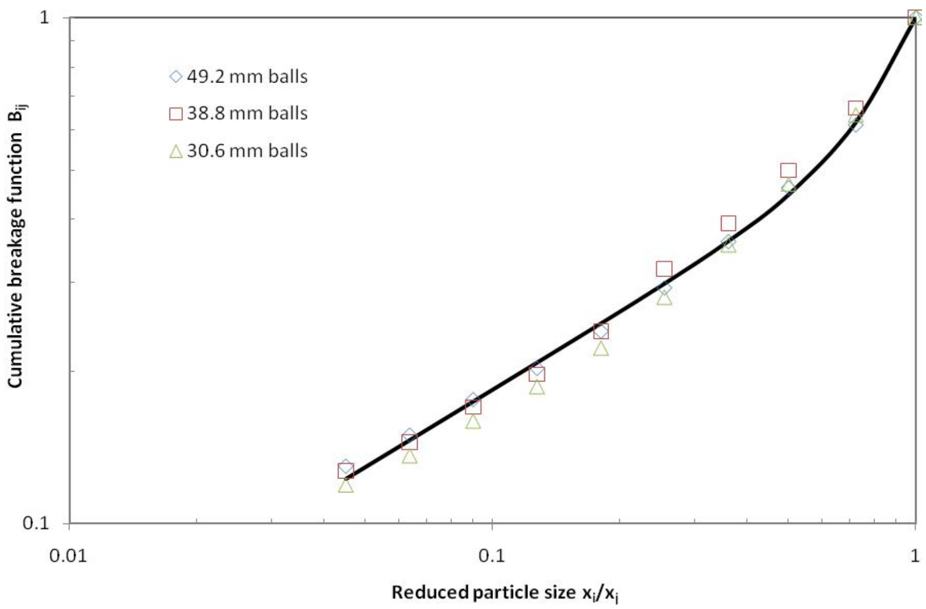

Figure 4.4 Reduced cumulative breakage function

A summary of the optimized parameters for each ball charge composition is presented in Table 4.2. The symbol *i* represents the interval index corresponding to each size class with the largest being $i = 1$.

Table 4.2 Breakage function parameters for different ball size distributions

	EQM-BSD			OEM-BSD			49.2 mm		38.8 mm	30.6 mm
i	**9**	**11**	**13**	**9**	**11**	**14**	**10**	**14**	**10**	**10**
β	2.8	3.1	3.5	3.1	3.0	3.5	3.2	3.5	2.9	3.0
γ	0.40	0.34	0.30	0.56	0.43	0.31	0.44	0.27	0.45	0.48
Φ	0.44	0.58	0.53	0.58	0.58	1.17	0.51	0.53	0.51	0.52

It can be seen that the parameter γ is very sensitive to milling conditions, that is, feed size and ball size distribution. To some extent, γ seems to increase with feed size. And the low γ values obtained suggest the fact that proportionally more fines are being produced from the breakage of the top size material. It is also an indication that the Tutuka coal is a soft material.

Talking about β and Φ, typical value ranges are generally found to be respectively 2.3 – 3.5 and 0.40 – 0.50 for coal (Austin *et al.*, 1984). In our investigation value ranges of 2.8 – 3.5 and 0.44 – 0.58 were found, which agree quite well with those reported above for Laurasian coals. It was however difficult to establish a trend between Φ values and ball size. This can be attributed to the fact that the 0.5 min grinding time was quite long for this particular coal. Because of this, the measurement of B_{ij} values was not precise enough for quantitative relations to be developed with accuracy.

Now, compared to Laurasian coals, values of Φ obtained with the Tutuka coal were quite high. One would argue that the fraction of daughter products that contribute to the finer fraction is high. As a result of this, a small proportion of the product tends to preserve parent size implying that this coal is softer to break than Laurasian ones.

Another feature of great important is breakage normalization. Values of B_{ij} are known to be dimensionally normalized if the value of Φ is constant for all breaking sizes. In our case, Φ values were found in the range 0.44 – 0.58 which show clearly that the Tutuka coal is non-normalizable. Nonetheless, if one assumes the material to be normalizable for simulation purposes – and as a result reduces the number of parameters – deviations in the order of 15 % are to be expected. Following this, it cannot be stated with confidence whether the Tutuka coal is normalizable or not. The best thing to do is to rather consider much shorter grinding time of the order of 10 – 15 seconds for future work. This will enable the data from coarser materials to also be used for breakage parameter estimation.

Finally, it should be noted that the data from Table A.19 in the Appendix is completely out of line and appears to be incorrect. That is why, it has not been used for breakage parameter estimation. It is therefore believed that the difficulties in obtaining close sized fractions and in producing representative samples at finer feed sizes have something to do with this. Similar discrepancies were also noticed for Table A.11 and A.26.

4.5 Significance of results (Interpretation)

The dependency of *a*-values on ball diameter *d* is best described using Equation (10) in which ξ=1 as presented in literature (Austin *et al.*, 1984). But earlier laws defined the competent media as the size of the ball corresponding to the maximum rate of breakage for a given size of particle. The following empirical equation was used:

$$x_m = K.d^{\eta} \tag{4.4}$$

This equation is generalized based upon Equations (2.9) and (2.11) in which α, Λ, a_0, μ_0, and d_0 are constant. Moreover, Equation (2.9) shows that x_m is directly proportional to μ making no difference in the use of x_m in lieu of μ in the analysis.

Austin *et al.* (1976) reported that the competent ball size was determined using Equation (4.4) in which η=2. Interestingly, the value of η was found to be 2 for the Tutuka coal.

Kelsall *et al.* (1967) proposed η=2 based on experiments done on quartz material. They reported in fact that this exponent was used for decades as an empirical way of choosing the competent ball diameter. Austin *et al.* (1984) also found a value of 2 based on experiment they did on coal.

Yildirim *et al.* (1999) in their particular case found that η=1 simulated reasonably well a dry grinding circuit of quartz. Recently, Austin *et al.* (2006) substituted 1.2 for η on an iron ore.

On their side, Kotake *et al.* (2004) were able to show that η is relatively larger for synthesized silica glass than for other materials they used. On average, they reported values between 0.89 and 1.42. The most important point is that they believed these discrepancies could be a result of inherent properties of the materials used such as density, Mohs hardness, Vicker’s hardness, Young’s modulus, and Poisson’s ratio.

This suggests that the exponent factor η is clearly not a predefined constant parameter. It might primarily depend on the material used. For this reason, it is justifiable to estimate it depending on the laboratory conditions.

Ultimately, no straightforward reason can be given to elucidate the different η-values reported. But it seems to us that this exponent factor is material-dependent. Only a detailed and systematic investigation will tell more on this hypothesis.

4.6 Summary

Equation (2.7) works very well providing the correction factor is given by Equation (2.8). Conversely, Equation (2.15) seems not to work at all here. Austin *et al.* (1986) also reached the same conclusion.

As far as the selection function equation is concerned, Equation (2.8) is entirely adequate as correction factor and seems to be the best model for the limited amount of information available at hand.

As for the breakage function, it has revealed the material to be non-normalizable. However, within 15 % deviation, the Tutuka coal can still be considered normalizable. And until more information is made available, not much can be done as to modelling the breakage function. At least, at this point in time, the proportional variation of γ and Φ presented in Table 4.2 can be used in preliminary simulations. But one needs to bear in mind that for qualitative works, complex models may be required especially with naturally-occurring minerals like the coal under consideration. This can be possible only when a well-thought laboratory work plan intended towards measuring the breakage function parameters is devised.

More importantly, published values of η so far range between 1 and 2. With the high value of the factor η found in this case study, the ball size effect reveals that this coal will be very sensitive to the ball size distribution inside the mill. Such an anticipated statement is evaluated in the next chapter.

Chapter 5 Effect of ball size distribution on milling kinetics

Single sizes of balls used for breakage parameter estimation do not represent at all the ball size distribution of an industrial mill even at start-up. For that reason, true validation of the milling process comes from the tests that mimic a real ball mixture.
For that reason, two ball size distributions were tested and the results obtained compared to the prediction using appropriate models.
In this chapter, raw data corresponding to two ball mixtures are manipulated in order to get a reasonable description of the effect of ball size distribution on breakage rate of a South African coal. This information can in future be used in the scale-up of laboratory results or simulated behaviour of various ball mixtures for industrial applications.

5.1 Introduction

The choice of media charge composition that optimizes ball milling circuits has had significant financial implications. This problem has been industrially addressed using a trial-and-error approach coupled with experience. Mill performance and ball size distribution are so intimately related that it is crucial to better understand their interrelation. This will then orientate process engineers in choosing the optimal ball mixture.
For the first time, Concha *et al.* (1992) proposed a remarkable algorithm that can be used to optimize the ball charge composition under defined operating constraints. This method relies on batch laboratory tests. These tests are used to characterize the grinding properties of the material being studied. The amount of laboratory work required to fully characterize the mineral matter is considerable. Tests are lengthy, tedious, and physically-challenging. Additionally, batch tests are carried out on several narrow particle size classes using single ball sizes. To have an estimate of the

overall effect of a mixture of balls in the mill, one must measure it on a well defined ball size distribution. In latter case, the data obtained will be valid for the considered ball mixture which should be similar to that used in the industrial mill. At present, no model is available that fully predicts the behaviour of a ball mix without relying upon results of batch tests for single ball sizes.

Typically, at least three single ball sizes are needed to unambiguously model the effect of ball diameter on milling rate. Then, a mix of balls can also be tested to mimic for example a real ball size distribution of an industrial plant. This set of information is then incorporated in the simulation model to obtain the optimum charge composition.

The core of this chapter focuses on investigating the effect of ball size distribution on the milling properties of the Tutuka coal. The sensitivity of the milling rate with the ball size distribution is examined to get much insight on the dependence of breakage rate of coal on the ball size distribution.

5.2 Selection function of ball mixtures

Milling rates are investigated for two charge mixes. Then, the measured rates are compared to the predicted ones. Finally, the discrepancies are discussed.

5.2.1 Equilibrium ball size distribution

Equation (2.30) shows that the equilibrium charge consists of an equal number of balls in each ball class providing the class widths are the same. In other words, according to Bond law, the equilibrium ball charge distribution is in statistical terms a constant number distribution function. This property was used to prepare the first charge mass denoted here EQM-BSD. Distributions in terms of mass and number fractions are presented in Figures 5.1 and 5.2 along with the second ball charge which will be discussed in the next sub-section.

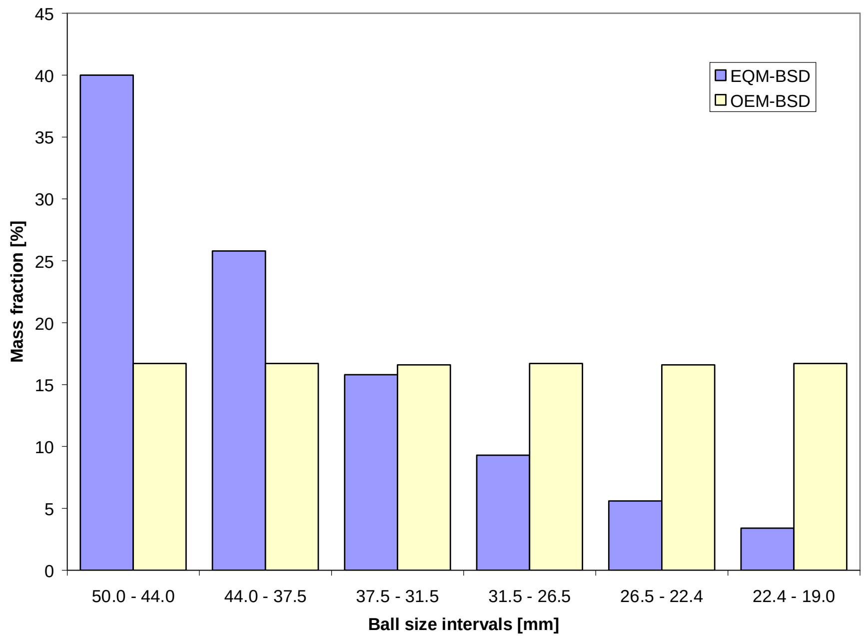

Figure 5.1 EQM and OEM ball mass size distributions used

5.2.2 Original equipment manufacturer recommended ball size distribution

According to GEC ALSTHOM Stein Industries, the manufacturer of the ball mills currently operating at Tutuka Power Station, the optimal performance of the mills is recorded for a constant mass size distribution function of the load. For this reason, the second charge mixture was prepared with this recommendation in mind.

The two ball size distributions used are compared as shown in Figure 5.1 and 5.2 on the mass fraction and number bases respectively.

The OEM-BSD considers the same mass of balls in the different ball size classes. The distribution therefore implies more balls of small sizes as a consequence of the defined distribution (Figure 5.2). This increases the total surface area of the load; and thereby, an increase in the rate of production of fine particles is expected. On the other hand, the low number of bigger balls limits the competence of the OEM load in breaking larger particles.

By contrast, the EQM-BSD would exhibit more competence for coarser particles than fines.

In sum, EQM-BSD encourages breakage by impact whereas OEM-BSD induces more breakage by abrasion and attrition.

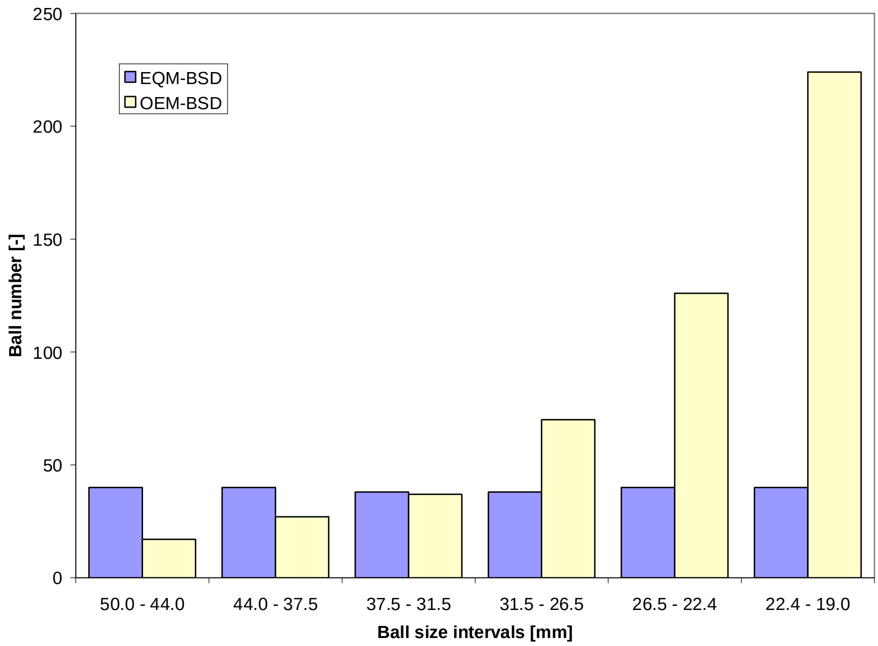

Figure 5.2 EQM and OEM ball number size distributions used

5.3 Results and discussion

In this section, the selection functions under both OEM- and EQM-BSD's as produced from the batch grinding test are compared to the predictions.

5.3.1 Ball size distribution effect

In order to study the effect of ball size distribution on milling rate, a single equation encompassing the breakage parameters, the effect of ball size and the overall selection function for a charge mix was to be produced.

With reference to Equations (2.2), (2.10), (2.11), and (2.31), the following was derived

$$\overline{S_i} = a_0 x_i^{\alpha} \cdot \sum_{k=1}^{n} \frac{m_k (d_0/d_k)^{\xi}}{1 + \left[\dfrac{x_i}{\mu_0 (d_k/d_0)^{\eta}} \right]^{\Lambda}} \tag{5.1}$$

where a_0 and μ_0 are the fitted values from laboratory test results. In this work a_0 and μ_0 obtained from d_0=38.8 mm balls are used. This is due to the fact that this ball diameter covers at the same time the normal and abnormal breakage regions.

Fixing ξ=1 (Austin *et al.*, 1984; Austin *et al.*, 2006) because it is reported to satisfactorily reflect to the effect of ball diameter on a (Equation 2.10), the single parameter η was estimated by regression to the data from the EQM-BSD tests. Its value was found to be 1.96 which is comparable to the one found in the section 4.3, i.e. η=2.

The results of the findings are depicted in Figure 5.3 where predictions are compared to measured rates of breakage.

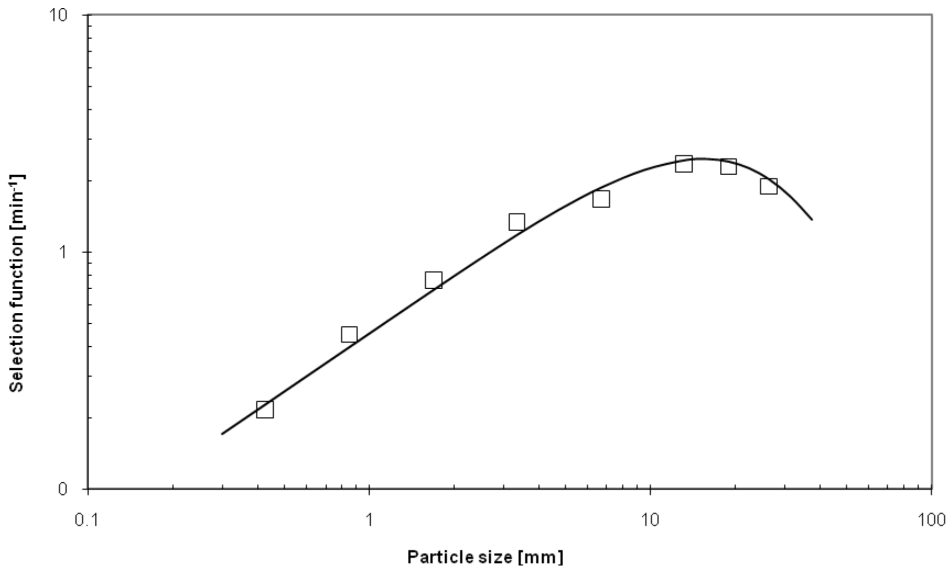

Figure 5.3 EQM-BSD graph as predicted with Equation (5.1)

As it can be seen, the results compare well and on average the discrepancies recorded are in the order of 5 – 10 %.

5.3.2 Validation of ball mixture model

To validate the values of ξ and η found in the previous sub-section, another attempt to predict milling performance on the OEM-BSD was initiated. To do this, 38.8 mm ball was again the starting point, i.e. a_0=0.48 and μ_0=19.27.

To fully predict the performance of the ball mix, Equation (5.1) was once more used. Given the ball distribution (Table 3.2), 38.8 mm breakage parameters (Table 4.1) and ξ=1 and η=2 (rounded off values), $\overline{S_i}$ for the OEM-BSD was calculated.

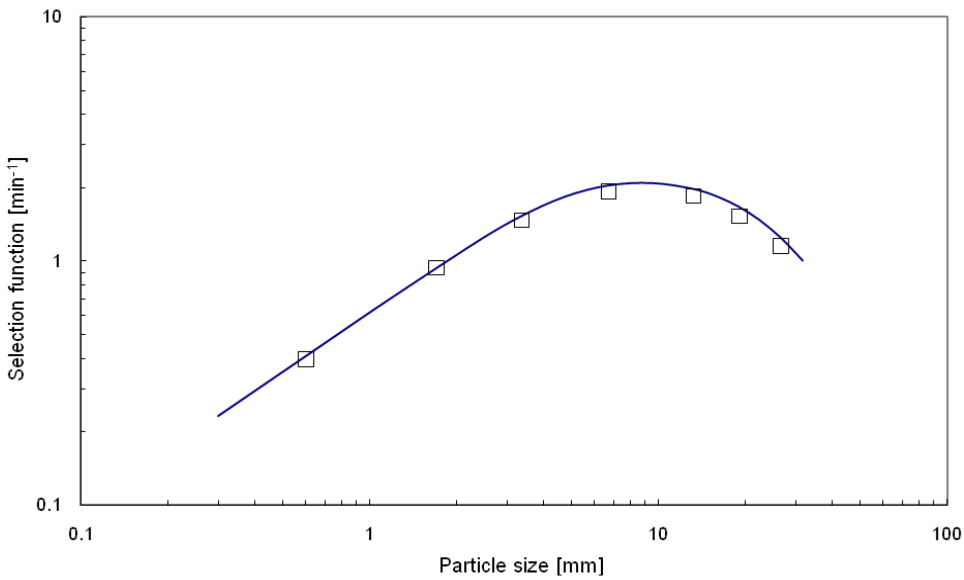

Figure 5.4 Comparison of the predicted and measured selection on OEM-BSD

Figure 5.4 shows a comparison of the lab results and the prediction of OEM-BSD for the following exponent factors: η=2 and ξ=1.

Here again, the questioned value of η turns out to be in agreement with the fixed value of approximately 2 since an average deviation of not much than 5% in the predictions is found especially in the normal breakage region.

5.3.3 Significance of findings

As mentioned in sub-section 5.2.2 above, Figure 5.5 appears to be in line with the expectations. By the same token, OEM-BSD is efficient up to about 7 mm coal size, then is overtaken by EQM-BSD at coarser coal sizes. Shift from EQM-BSD to OEM-BSD at coal size below 7 mm brings an increase in the milling rate of 20% on average, whereas doing it the other way round for sizes greater than 7 mm improves the milling rate by about 45 %.

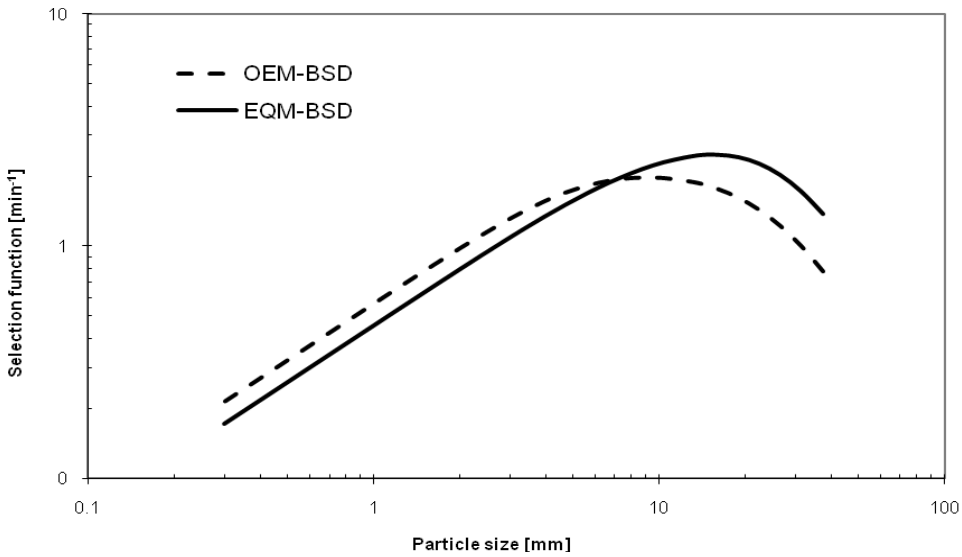

Figure 5.5 Modelled kinetics of the ball size distributions

Eventually, the accuracy of the predictions against the results was computed. At this point, the coefficient of determination and the standard error of estimate were used to assess the goodness of the fits. Triola (2005) defines the coefficient of determination as the amount of the variation in the dependent variable (often refer to as the *y*-

variable) that is explained by the regression line with respect to the predictor variable. Known also as the R-squared value, it is a way of evaluating the quality of a curve fit. As a rule of thumb, Palm (2001) recommends a value of $r^2 \geq 0.99$; in other words, a fit is good if it accounts for at least 99 % of the data variation. However, for practical applications, Triola (2005) argues that a value of $r^2 \geq 0.95$ is the standard accepted by statisticians worldwide.

In discussing this matter further, the definition given by Triola (2005) would be a good starting point.

For a collection of paired data containing of sample points (x,y), if y_{mdl} is defined as the predicted value of y (obtained by using the regression equation), and $\bar{y}$ as the mean of the sample y-values, the following can be deduced:

1° The explained deviation is the vertical distance $y_{mdl} - \bar{y}$, which is the distance between the predicted y-value and the horizontal line passing through the sample mean $\bar{y}$.

2° The unexplained deviation is the vertical distance $y - y_{mdl}$, which is the vertical distance between the point (x,y) and the regression line. This distance $y - y_{mdl}$ is also called residual.

3° The total deviation (from the mean) of the particular point (x,y) is the vertical distance $y - \bar{y}$, which is the distance between the point (x, y) and the horizontal line passing through the sample mean $\bar{y}$.

With reference to the above, the coefficient of determination is defined as

$$r^2 = \frac{\text{Explained variation}}{\text{Total variation}} \tag{5.2}$$

where the total variation represents the sum of the squares of the total deviation values and the explained variation is the sum of the squares of the explained deviation values.

In order to determine the accuracy of a predicted value, the notion of prediction interval is brought up, which is an interval estimate of a predicted value of y. From there, the spread of sample points about the regression line and the average error of estimate can be calculated.

The standard error of estimate, denoted by s_e, represents a measure of the differences (or distances) between the observed sample y-values and the predicted values y_{mdl} that are obtained using the regression equation. It is given by (Triola, 2005)

$$s_e = \sqrt{\frac{\sum (y - y_{mdl})^2}{N - 2}} \tag{5.3}$$

where y_{mdl} is the predicted y-value and N is the number of sample points.

In this case study, it was found that:

- For the EQM-BSD, r^2=0.977 and the average error of estimate was 9.18 %
- and for the OEM-BSD, r^2=0.986 and the average error of estimate was 4.89 %.

Though high coefficients of determination are found, they cannot provide good answers to the underlying engineering or scientific questions under investigation. Nevertheless Equation (5.1) approximates the measured data points very well.

5.4 Summary

Two ball charge mixtures were compared. It was found as expected that on the one hand the selection function graph corresponding to the EQM-BSD lies below the OEM-BSD one at lower particle sizes; and on the other hand, it increases continuously and becomes higher for coarser sizes.

Equation (5.1) which gives an estimate of the overall value of breakage rate for a ball mixture in the mill accurately describes the ball size distribution effect. With ξ (the factor which relates a to d) and η (the factor which relates μ to d) estimated in the previous chapter to be respectively 1 and 2, the selection function for the ball size mixture can be reasonably predicted with an average deviation of 5 – 10 %.

Chapter 6 Conclusion

6.1 Introduction

A coal from Tutuka Power coal was characterized in the Minerals Processing Laboratory of the University of the Witwatersrand. The principal objective was to determine the ball size and ball size distribution effects on the selection function for future optimization of the mill ball charge. The breakage function was also studied but not in as much detail as the selection function.

The outcomes of the investigation are summarized here. They constitute the first step in the assessment of South African coals in general for milling applications.

6.2 Summary of findings

6.2.1 Ball size effect

Not enough information could be produced to estimate precisely the parameter Λ. Because of this, a default value of 3 was used (Austin *et al.*, 1984). Despite the uncertainty, the predictions agreed well with the real data. The different breakage parameters are summarized in Table 6.1.

Table 6.1 Tutuka coal breakage characteristics

Selection function parameters		Breakage function parameters	
α	0.81	β	3.2
Λ	3	γ	0.53
ξ	1	Φ	0.44 – 0.58
η	2	**Non-normalizable**	

Even though the primary breakage distribution function was not studied in much detail, the preliminary calculations suggested that the coal could be considered non-normalizable. A more elaborated laboratory work plan intended towards measuring accurately the breakage function parameters is required in future. Until this work is systematically carried out, estimations given in Table 6.1 will be used as such for preliminary simulations.

As for the breakage function parameters, the low value of γ is an indication that the Tutuka coal is a very soft material.

On another note, Equations (2.14) and (2.15) were tried out. In spite of the fact that the laboratory results seems to display a trend, Snow's equations could not fit the data well. To a large extent, Snow's equations (2.14) and (2.15) do not approximate at all the selection function values measured.

6.2.2 Ball size distribution effect

This study has revealed that an increase of 20 – 45 % in the selection function is achievable by increasing the proportion of small balls in the mill charge. It has also shown that South African coals are very sensitive to the ball charge mix. Therefore, the optimization of the ball mix by simulation will always require confidence in the model parameters to input to the simulator. Also observed, the overall breakage rate due to a ball size mixture can be predicted from tests on a few individual ball sizes.

6.3 Overall conclusion

The breakage properties of a South African coal were estimated and the effect of ball size and ball size distribution deduced. An equation encompassing at the same time ball size and ball size distribution effects for parameter search was tested. It was found that the equation can be used for parameter estimation of the breakage properties of materials.

In the final analysis, it was noted in particular that ξ (the factor which relates a to d) proves to be close to 1. The factor η (the factor which relates μ to d), on the other hand, is ostensibly material dependent. But the η-value of 2 satisfactorily simulates the behaviour of coal. Fixing a priori the value of η is therefore inadequate. It should rather be deduced from tests on at least two ball sizes which are substantially different, e.g. 30 and 50 mm. As to whether parameter η is material dependent or not, only future research will tell. This will require more tests in the abnormal region to confidently estimate the parameter Λ.

References

Austin, L.G., Bagga, P., Celik, M., 1981. Breakage properties of some materials in a laboratory ball mill, *Powder Technology*, vol. 28, no. 2, pp. 235 – 241

Austin, L.G., Bhatia, V.K., 1971/72. Experimental methods for grinding studies in laboratory mills, *Powder Technology*, vol. 5, no. 5, pp 261 – 266

Austin, L.G., Brame, K., 1983. A comparison of Bond method for sizing wet tumbling ball mills with a size-mass balance simulation model, *Powder Technology*, vol. 34, no. 2, pp. 261 – 274

Austin, L.G., Julianelli, K., de Souza, A.S., Schneider, C.L., 2006. Simulation of wet ball milling of iron ore at Carajas – Brazil, *International Journal of Mineral Processing*, vol. 84, no. 1 – 4, pp. 157 – 171

Austin, L.G., Klimpel, R.R., 1985. Ball wear and ball size distribution in tumbling mills, *Powder Technology*, vol. 41, no. 3, pp. 279 – 286

Austin, L.G., Klimpel, R.R., Luckie, P.T., 1984. Process Engineering of Size Reduction: Ball Milling, *AIME-SME*, New York, USA

Austin, L.G., Luckie, P.T., 1971/72. Methods for determination of breakage distribution parameters, *Powder Technology*, vol. 5, no. 4, pp 215 – 222

Austin, L.G., Shoji, K., Everett, M.D., 1973. An explanation of abnormal breakage of large particle sizes in laboratory mills, *Powder Technology*, vol. 7, no. 1, pp 3 – 7

Austin, L.G., Shoji, K., Bell, D., 1982. Rate equations for non-linear breakage in mills due to material effects, *Powder Technology*, vol. 31, no. 1, pp. 127 – 133

Austin, L.G., Shoji, K., Luckie, P.T., 1976. The effect of ball size on mill performance, *Powder Technology*, vol. 14, no. 1, pp. 71 – 79

Austin, L.G., Trimarchi, T., Weymont, N.P., 1977. An analysis of some cases of non-first-order breakage rates, *Powder Technology*, vol. 17, no. 1, pp. 109 – 113

Bazin, C., 2005. Data reconciliation for the calibration of a model for batch grinding, *Minerals Engineering*, vol. 18, no. 10, pp. 1052 – 1056

Cleary, P.W., 2001. Charge behaviour and power consumption in ball mills: sensitivity to mill operating conditions, liner geometry and charge composition, *International Journal of Mineral Processing*, vol. 63, no. 2, pp. 79 – 114

Concha, F., Magne, L., Austin, L.G., 1992. Optimization of the make-up ball charge in a grinding mill, *International Journal of Mineral Processing*, vol. 34, no. 3, pp. 231 – 241

Falcon, L.M., Falcon, R.M.S., 1987. The petrographic composition of Southern African coals in relation to friability, hardness, and abrasive indices, *Journal of the South African Institute of Mining and Metallurgy*, vol. 87, no. 10, pp. 323 – 336

Falcon, R., Ham, A.J., 1988. The characteristics of Southern African coals, *Journal of the South African Institute of Mining and Metallurgy*, vol. 88, no. 5, pp. 145 – 161

Gardner, R.P., Austin, L.G., 1975. The applicability of the first-order grinding law to particles having a distribution of strengths, *Powder Technology*, vol. 12, no. 1, pp. 65 – 69

Gupta, A., Yan, D.S., 2006. Mineral Processing Design and Operation: An introduction, *Elsevier*, ISBN: 978-0-4444-51636-7

Gupta, V.K., Zouit, H., Hodouin, D., 1985. The effect of ball and mill diameters on grinding rate parameters in dry grinding operation, *Powder Technology*, vol. 42, no. 2, pp. 199 – 208

Hukki, R.T., 1954. Correlation between principal parameters affecting mechanical ball wear, *Mining Engineering*, pp. 642 – 644

Kelly, E.G., Spottiswood, D.J., 1990. The breakage function; What is it really?, *Minerals Engineering*, vol. 3, no. 5, pp. 405 – 414

Kelly, E.G., Spottiswood, D.J., 1982. Introduction to Mineral Processing, *John Wiley & Sons*, ISBN 0-471-03379-0, USA.

Kelsall, D.F., Stewart, P.S.B., Weller, K.R., 1973. Continuous grinding in a small wet ball mill. Part IV. A study of the influence of grinding media load and density, *Powder Technology*, vol. 7, no. 5, pp. 293 – 301

Kelsall, D.F., Reid, K.J., Restarick, C.J., 1967. Continuous grinding in a small wet ball mill. Part I. A study of the influence of ball diameter, *Powder Technology*, vol. 1, no. 5, pp. 291 – 300

King, R.P., 2001. Modeling and simulation of mineral processing systems, *Butterworth-Heinemann*, ISBN: 0-7506-4884-8

Kotake, N., Daibo, K., Yamamoto, T., Kanda, Y., 2004. Experimental investigation on a grinding rate constant of solid materials by a ball mill – effect of ball diameter and feed size, *Powder Technology*, vol. 143 – 144, pp. 196 – 203

Kotake, N., Suzuki, K., Asahi, S., Kanda, Y., 2002. Experimental study on the grinding rate constant of solid materials in a ball mill, *Powder Technology*, vol.122, no. 2 – 3, pp. 101 – 108

Lameck, N.N.S., 2006. Coal selection and breakage functions parameterization, *Internal Report*, University of the Witwatersrand, Johannesburg.

Lameck, N.N.S., 2006. Effects of grinding media shapes on ball mill performance, *Master of Science Dissertation*, University of the Witwatersrand, Johannesburg.

Menacho, J., Concha, F., 1986. Mathematical model for ball wear in grinding mills, I. Zero-order wear rate, *Powder Technology*, vol. 47, no. 1, pp. 87 – 96

Menacho, J., Concha, F., 1987. Mathematical model for ball wear in grinding mills, II. General solution, *Powder Technology*, vol. 52, no. 3, pp. 267 – 277

Moys, M.H., 1984. The measurement of parameters describing behaviour of the load in a grinding mill, Mintek 50, *Proceedings of International Conference on Mineral Science and Technology*, Sandton, South Africa, pp. 205 – 219

Napier-Munn, T.J., Morrell, S., Morrison, R.D., Kojovic, T., 1999. Mineral Comminution Circuits: Their Operation and Optimization. *JKMRC*, Queensland, Australia

Nomura, S., Hosoda, K., Tanaka, T., 1991. An analysis of the selection function for mills using balls as grinding media, *Powder Technology*, vol. 68, no.1, pp. 1 – 12

Nomura, S., Tanaka, T., Callcott, T.G., 1994. The effect of mill power on the selection function for tumbling and vibration ball mills, *Powder Technology*, vol. 81, no.2, pp. 101 – 109

Palm, W.J., 2001. Introduction to Matlab 6 for Engineers, *McGraw-Hill*, Boston, USA

Powell, M.S., Morrison, R.D., 2007. The future of comminution modeling, *International Journal of Mineral Processing*, vol. 84, no. 1 – 4, pp. 228 – 239

Triola, M.F., 2005. Essentials of Statistics, Second Edition, *Pearson Addison-Wesley*, ISBN: 0-201-77129-2

Vermeulen, L.A., 1986. A contribution to 'Ball wear and ball size distribution in tumbling mills', *Powder Technology*, vol. 46, no. 2 – 3, pp. 281 – 285

Wills, B.A., 1992. Mineral Processing Technology: An Introduction to the Practical Aspects of Ore Treatment and Mineral Recovery, Fifth Edition. *Pergamon*

Yildirim, K., Austin, L.G., 1998. The abrasive wear of cylindrical grinding wear, *Wear*, vol. 218, no. 1, pp. 15 – 20

Yildirim, K., Cho, H., Austin, L.G., 1999. The modeling of dry grinding of quartz in tumbling media mills, *Powder Technology*, vol. 105, no. 1 – 3, pp. 210 – 221

Appendices

A Results of particle size analysis

A.1 Batch grinding tests on single ball sizes

In this section, the particle size distributions of the material as obtained after batch grinding are presented. They refer to tests performed using single sizes of balls, namely 30.6 mm, 38.8 mm, and 49.2 mm respectively.

A.1.1 Particle size distributions obtained using 30.6 mm balls

Table A.1 Results of size analysis for + 16000 – 13200 microns coal

Screen size (microns)	16000 microns		0.5 min		1 min		2 min	
	Retained	Passing	Retained	Passing	Retained	Passing	Retained	Passing
16000	0.00	100	0.00	100	0.00	100	0.00	100
13200	91.70	8.30	18.30	81.70	9.05	90.95	3.52	96.48
9500	8.28	0.02	30.13	51.56	22.08	68.87	13.41	83.07
6700	0.02	0.00	15.26	36.30	14.76	54.11	9.02	74.05
4700	0.00	0.00	8.34	27.96	9.34	44.77	7.32	66.73
3350	0.00	0.00	5.69	22.26	6.99	37.78	6.34	60.39
2360	0.00	0.00	4.16	18.10	5.60	32.18	5.91	54.48
1700	0.00	0.00	2.84	15.26	4.28	27.90	5.20	49.28
1180	0.00	0.00	2.90	12.36	4.55	23.35	5.91	43.37
850	0.00	0.00	1.85	10.51	3.09	20.26	4.85	38.53
600	0.00	0.00	1.70	8.80	3.15	17.11	5.11	33.41
425	0.00	0.00	1.46	7.35	2.78	14.33	5.03	28.38
300	0.00	0.00	1.37	5.98	2.73	11.61	5.11	23.27
212	0.00	0.00	1.01	4.97	2.04	9.57	4.06	19.21
150	0.00	0.00	0.85	4.12	1.70	7.86	3.40	15.81
106	0.00	0.00	0.77	3.35	1.57	6.29	3.22	12.59
75	0.00	0.00	0.56	2.79	1.17	5.12	2.36	10.24
Pan	0.00		2.79		5.12		10.24	

Table A.2 Results of size analysis for + 9500 – 6700 microns coal

Screen size (microns)	9500 microns		0.5 min		1 min		2 min	
	Retained	Passing	Retained	Passing	Retained	Passing	Retained	Passing
9500	0.00	100	0.00	100	0.00	100	0.00	100
6700	97.06	2.91	29.37	70.63	13.63	86.37	4.53	95.47
4700	2.84	0.07	22.39	48.24	17.00	69.37	7.24	88.24

3350	0.07	0.00	13.32	34.92	13.02	56.35	8.30	79.94
2360	0.00	0.00	8.35	26.56	11.13	45.21	8.33	71.61
1700	0.00	0.00	5.15	21.41	7.16	38.05	7.75	63.86
1180	0.00	0.00	4.52	16.89	7.01	31.05	9.05	54.82
850	0.00	0.00	2.80	14.09	4.66	26.38	7.07	47.74
600	0.00	0.00	2.45	11.64	4.51	21.87	7.22	40.52
425	0.00	0.00	2.04	9.60	3.75	18.12	6.70	33.83
300	0.00	0.00	1.84	7.76	3.54	14.58	6.41	27.42
212	0.00	0.00	1.34	6.43	2.61	11.97	4.84	22.58
150	0.00	0.00	1.07	5.36	2.17	9.80	4.06	18.52
106	0.00	0.00	0.98	4.37	1.99	7.81	3.80	14.72
75	0.00	0.00	0.72	3.65	1.44	6.37	2.80	11.91
Pan	0.00		3.65		6.37		11.91	

Table A.3 Results of size analysis for + 2360 – 1700 microns coal

Screen size (microns)	**2360 microns**		**0.5 min**		**1 min**		**4 min**	
	Retained	**Passing**	**Retained**	**Passing**	**Retained**	**Passing**	**Retained**	**Passing**
2360	0.00	100	0.00	100	0.00	100	0.00	100
1700	93.52	6.48	50.40	49.60	27.86	72.14	1.13	98.87
1180	6.23	0.25	16.69	32.90	18.70	53.44	4.60	94.27
850	0.25	0.00	7.75	25.15	11.07	42.37	7.40	86.87
600	0.00	0.00	5.42	19.74	8.77	33.60	10.10	76.77
425	0.00	0.00	3.83	15.90	6.63	26.97	10.35	66.42
300	0.00	0.00	3.06	12.85	5.48	21.49	10.77	55.66
212	0.00	0.00	1.94	10.90	3.62	17.87	8.29	47.36
150	0.00	0.00	1.51	9.40	2.87	14.99	7.40	39.97
106	0.00	0.00	1.31	8.08	2.56	12.43	7.22	32.75
75	0.00	0.00	0.97	7.11	1.87	10.56	5.46	27.28
Pan	0.00		7.11		10.56		27.28	

A.1.2 Particle size distributions obtained using 38.8 mm balls

Table A.4 Results of size analysis for + 26500 – 22400 microns coal

Screen size (microns)	**26500 microns**		**0.5 min**		**1 min**		**2 min**	
	Retained	**Passing**	**Retained**	**Passing**	**Retained**	**Passing**	**Retained**	**Passing**
26500	0.00	100	0.00	100	0.00	100	0.00	100
22400	92.77	7.23	19.40	80.60	7.05	92.95	1.09	98.91
19000	7.23	0.00	16.39	64.20	14.16	78.79	2.19	96.72
16000	0.00	0.00	14.77	49.43	10.95	67.84	4.34	92.38

13200	0.00	0.00	4.32	45.11	5.09	62.75	5.53	86.85
9500	0.00	0.00	10.76	34.35	9.16	53.59	10.18	76.67
6700	0.00	0.00	6.38	27.98	7.87	45.72	9.37	67.30
4700	0.00	0.00	4.19	23.79	5.20	40.53	7.13	60.17
3350	0.00	0.00	3.37	20.42	4.80	35.72	6.43	53.74
2360	0.00	0.00	3.07	17.35	4.46	31.26	4.77	48.97
1700	0.00	0.00	2.37	14.98	3.71	27.54	5.86	43.11
1180	0.00	0.00	2.49	12.49	4.42	23.13	5.05	38.06
850	0.00	0.00	1.77	10.72	3.20	19.92	4.91	33.15
600	0.00	0.00	1.71	9.01	3.16	16.76	5.24	27.91
425	0.00	0.00	1.51	7.50	2.92	13.84	3.78	24.13
300	0.00	0.00	1.41	6.10	2.79	11.05	3.45	20.68
212	0.00	0.00	1.14	4.95	1.76	9.29	3.16	17.52
150	0.00	0.00	0.84	4.11	1.75	7.54	2.92	14.60
106	0.00	0.00	0.81	3.30	1.62	5.92	2.99	11.61
75	0.00	0.00	0.59	2.71	1.19	4.73	2.56	9.05
Pan	0.00		2.71		4.73		9.05	

Table A.5 Results of size analysis for + 16000 – 13200 microns coal

Screen size (microns)	**16000 microns**		**0.5 min**		**1 min**		**2 min**	
	Retained	**Passing**	**Retained**	**Passing**	**Retained**	**Passing**	**Retained**	**Passing**
16000	0.00	100	0.00	100	0.00	100	0.00	100
13200	96.36	3.64	16.26	83.74	7.90	92.10	1.05	98.95
9500	3.64	0.00	25.78	57.96	16.60	75.50	6.10	92.85
6700	0.00	0.00	15.11	42.85	13.57	61.93	5.13	87.72
4700	0.00	0.00	9.30	33.55	9.70	52.23	6.89	80.83
3350	0.00	0.00	6.59	26.96	7.48	44.75	6.78	74.05
2360	0.00	0.00	4.91	22.05	6.86	37.89	8.32	65.73
1700	0.00	0.00	3.59	18.46	5.26	32.63	8.97	56.76
1180	0.00	0.00	3.62	14.84	5.63	27.00	8.89	47.87
850	0.00	0.00	2.34	12.50	4.06	22.94	8.05	39.82
600	0.00	0.00	2.11	10.39	3.85	19.09	6.28	33.54
425	0.00	0.00	1.80	8.59	3.38	15.71	5.74	27.80
300	0.00	0.00	1.62	6.97	3.16	12.55	4.99	22.81
212	0.00	0.00	1.29	5.68	2.40	10.15	3.43	19.38
150	0.00	0.00	0.93	4.75	1.94	8.21	3.69	15.69
106	0.00	0.00	0.91	3.84	1.77	6.44	3.02	12.67
75	0.00	0.00	0.66	3.18	1.29	5.15	2.61	10.06
Pan	0.00		3.18		5.15		10.06	

Table A.6 Results of size analysis for + 6700 – 4750 microns coal

Screen size (microns)	6700 microns		0.5 min		1 min		1.5 min	
	Retained	**Passing**	**Retained**	**Passing**	**Retained**	**Passing**	**Retained**	**Passing**
6700	0.00	100	0.00	100	0.00	100	0.00	100
4700	94.76	5.24	34.49	65.51	14.99	85.01	7.17	92.83
3350	5.24	0.00	20.05	45.46	16.64	68.37	10.54	82.30
2360	0.00	0.00	12.73	32.73	14.13	54.23	12.46	69.84
1700	0.00	0.00	7.29	25.44	10.06	44.17	10.32	59.51
1180	0.00	0.00	6.05	19.39	9.16	35.01	11.24	48.27
850	0.00	0.00	3.54	15.85	6.06	28.95	8.01	40.26
600	0.00	0.00	2.98	12.87	5.30	23.65	7.44	32.82
425	0.00	0.00	2.40	10.48	4.33	19.32	6.32	26.50
300	0.00	0.00	1.95	8.52	3.80	15.51	5.53	20.97
212	0.00	0.00	1.53	6.99	2.82	12.70	4.20	16.77
150	0.00	0.00	1.11	5.89	2.25	10.45	3.28	13.48
106	0.00	0.00	1.06	4.82	2.03	8.41	3.06	10.42
75	0.00	0.00	0.78	4.05	1.49	6.92	2.14	8.28
Pan	0.00		4.05		6.92		8.28	

Table A.7 Results of size analysis for + 2360 – 1700 microns coal

Screen size (microns)	2360 microns		0.5 min		1 min		2 min	
	Retained	**Passing**	**Retained**	**Passing**	**Retained**	**Passing**	**Retained**	**Passing**
2360	0.00	100	0.00	100	0.00	100	0.00	100
1700	95.27	4.73	53.69	46.31	30.01	69.99	10.18	89.82
1180	4.73	0.00	14.72	31.59	19.12	50.87	16.22	73.60
850	0.00	0.00	6.72	24.87	10.19	40.68	12.03	61.57
600	0.00	0.00	4.75	20.12	8.12	32.56	11.15	50.42
425	0.00	0.00	4.52	15.60	6.20	26.36	9.13	41.29
300	0.00	0.00	2.78	12.82	4.92	21.44	7.93	33.35
212	0.00	0.00	1.81	11.01	3.82	17.61	6.11	27.24
150	0.00	0.00	1.61	9.40	2.82	14.80	4.77	22.47
106	0.00	0.00	1.42	7.98	2.48	12.32	4.33	18.14
75	0.00	0.00	0.95	7.03	1.86	10.46	3.24	14.91
Pan	0.00		7.03		10.46		14.91	

A.1.3 Particle size distributions obtained using 49.2 mm balls

Table A.8 Results of size analysis for + 22400 – 19000 microns coal

Screen size (microns)	22400 microns		0.5 min		1 min		2 min	
	Retained	Passing	Retained	Passing	Retained	Passing	Retained	Passing
22400	0.00	100	0.00	100	0.00	100		
19000	88.24	11.76	14.89	85.11	5.89	94.11		
16000	11.76	0.00	20.66	64.45	13.82	80.29		
13200	0.00	0.00	8.01	56.44	5.29	75.00		
9500	0.00	0.00	15.21	41.23	11.45	63.55		
6700	0.00	0.00	8.04	33.19	9.74	53.81		
4700	0.00	0.00	6.47	26.72	7.72	46.09		
3350	0.00	0.00	4.51	22.21	6.35	39.74		
2360	0.00	0.00	3.84	18.37	5.64	34.10		
1700	0.00	0.00	2.93	15.45	4.73	29.37		
1180	0.00	0.00	2.93	12.52	5.00	24.37		
850	0.00	0.00	1.99	10.53	3.65	20.72		
600	0.00	0.00	1.82	8.72	3.50	17.22		
425	0.00	0.00	1.56	7.15	3.10	14.12		
300	0.00	0.00	1.38	5.77	2.81	11.30		
212	0.00	0.00	1.12	4.65	2.29	9.02		
150	0.00	0.00	0.82	3.84	1.64	7.38		
106	0.00	0.00	0.78	3.06	1.59	5.79		
75	0.00	0.00	0.57	2.49	1.14	4.65		
Pan	0.00		2.49		4.65			

Table A.9 Results of size analysis for + 9500 – 6700 microns coal

Screen size (microns)	9500 microns		0.5 min		1 min		2 min	
	Retained	Passing	Retained	Passing	Retained	Passing	Retained	Passing
9500	0.00	100	0.00	100	0.00	100		
6700	94.10	5.90	26.39	73.61	9.31	90.69		
4700	5.90	0.00	21.19	52.42	14.93	75.76		
3350	0.00	0.00	13.47	38.95	13.55	62.21		
2360	0.00	0.00	8.68	30.28	11.12	51.09		
1700	0.00	0.00	5.90	24.38	8.79	42.30		
1180	0.00	0.00	5.54	18.84	8.73	33.57		
850	0.00	0.00	3.35	15.49	5.74	27.83		
600	0.00	0.00	2.77	12.72	5.07	22.76		

425	0.00	0.00	2.30	10.42	4.20	18.56		
300	0.00	0.00	1.93	8.49	3.58	14.98		
212	0.00	0.00	1.53	6.96	2.85	12.13		
150	0.00	0.00	1.13	5.83	2.05	10.08		
106	0.00	0.00	1.11	4.73	2.00	8.08		
75	0.00	0.00	0.83	3.90	1.45	6.63		
Pan	0.00		3.90		6.63			

Table A.10 Results of size analysis for + 2360 – 1700 microns coal

Screen size (microns)	**2360 microns**		**0.5 min**		**1 min**		**2 min**	
	Retained	**Passing**	**Retained**	**Passing**	**Retained**	**Passing**	**Retained**	**Passing**
2360	0.00	100	0.00	100	0.00	100	0.00	100
1700	97.24	2.76	56.17	43.83	33.24	66.76	12.20	87.80
1180	2.76	0.00	15.26	28.58	18.99	47.77	16.53	71.26
850	0.00	0.00	6.22	22.36	9.64	38.14	11.92	59.34
600	0.00	0.00	4.39	17.96	7.45	30.69	10.71	48.63
425	0.00	0.00	3.13	14.83	5.58	25.11	8.73	39.90
300	0.00	0.00	2.48	12.35	4.54	20.57	7.60	32.30
212	0.00	0.00	1.81	10.54	3.38	17.18	6.03	26.27
150	0.00	0.00	1.33	9.21	2.42	14.76	4.34	21.94
106	0.00	0.00	1.32	7.89	2.36	12.40	4.30	17.63
75	0.00	0.00	1.00	6.89	1.77	10.63	3.11	14.53
Pan	0.00		6.89		10.63		14.53	

Table A.11 Results of size analysis for + 600 – 425 microns coal

Screen size (microns)	**600 microns**		**0.5 min**		**1 min**		**2 min**	
	Retained	**Passing**	**Retained**	**Passing**	**Retained**	**Passing**	**Retained**	**Passing**
600	0.00	100	0.00	100	0.00	100	0.00	100
425	86.28	13.72	51.64	48.36	42.48	57.52	34.65	65.35
300	13.72	0.00	24.44	23.91	26.04	31.48	23.17	42.18
212	0.00	0.00	3.61	20.30	5.78	25.70	8.97	33.21
150	0.00	0.00	1.81	18.49	3.09	22.61	5.00	28.21
106	0.00	0.00	1.60	16.89	2.62	20.00	4.54	23.67
75	0.00	0.00	1.17	15.72	1.88	18.12	3.17	20.50
Pan	0.00		15.72		18.12		20.50	

A.2 Batch grinding tests on mixtures of balls

In this section, the particle size distributions of the material as obtained after batch grinding are presented. They refer to tests performed with the two ball size distributions, that is, EQM-BSD and OEM-BSD.

A.2.1 Particle size distributions obtained for the EQM-BSD

Table A.12 Results of size analysis for + 26500 – 22400 microns coal

Screen size (microns)	26500 microns		0.5 min		1 min		2 min	
	Retained	Passing	Retained	Passing	Retained	Passing	Retained	Passing
26500	0.00	100	0.00	100	0.00	100	0.00	100
22400	99.98	0.02	13.39	86.61	3.98	96.02	1.86	98.14
19000	0.00	0.02	18.74	67.87	11.21	84.81	5.77	92.37
16000	0.02	0.00	18.81	49.06	15.03	69.78	7.90	84.47
13200	0.00	0.00	6.02	43.04	6.10	63.68	4.11	80.36
9500	0.00	0.00	9.36	33.69	11.06	52.62	6.98	73.38
6700	0.00	0.00	6.65	27.04	8.33	44.29	6.28	67.11
4700	0.00	0.00	4.74	22.30	6.01	38.28	5.53	61.58
3350	0.00	0.00	3.28	19.02	4.83	33.45	4.76	56.82
2360	0.00	0.00	2.79	16.24	4.27	29.18	4.88	51.94
1700	0.00	0.00	2.10	14.13	3.36	25.82	4.42	47.52
1180	0.00	0.00	2.24	11.89	3.76	22.06	5.75	41.77
850	0.00	0.00	1.71	10.18	2.88	19.18	4.75	37.02
600	0.00	0.00	1.52	8.66	2.85	16.33	5.08	31.94
425	0.00	0.00	1.42	7.24	2.61	13.72	4.98	26.96
300	0.00	0.00	1.36	5.89	2.60	11.12	5.11	21.86
212	0.00	0.00	1.07	4.82	2.10	9.02	3.98	17.88
150	0.00	0.00	0.88	3.94	1.73	7.29	3.44	14.44
106	0.00	0.00	0.86	3.09	1.60	5.70	3.23	11.21
75	0.00	0.00	0.57	2.52	1.19	4.51	2.42	8.78
Pan	0.00		2.52		4.51		8.78	

Table A.13 Results of size analysis for + 19000 – 16000 microns coal

Screen size (microns)	19000 microns		0.5 min		1 min		2 min	
	Retained	Passing	Retained	Passing	Retained	Passing	Retained	Passing
19000	0.00	100	0.00	100	0.00	100	0.00	100
16000	97.57	2.43	20.95	79.05	6.65	93.35	1.48	98.52

13200	2.42	0.00	14.95	64.10	6.93	86.42	2.71	95.81
9500	0.00	0.00	19.73	44.37	16.52	69.90	8.28	87.53
6700	0.00	0.00	7.74	36.63	13.01	56.89	7.46	80.07
4700	0.00	0.00	11.12	25.51	8.42	48.47	6.40	73.67
3350	0.00	0.00	5.03	20.48	7.67	40.80	6.12	67.55
2360	0.00	0.00	4.38	16.10	5.72	35.08	6.92	60.63
1700	0.00	0.00	3.02	13.08	4.72	30.36	5.81	54.82
1180	0.00	0.00	3.03	10.05	5.16	25.20	7.68	47.13
850	0.00	0.00	2.21	7.84	3.59	21.60	5.96	41.17
600	0.00	0.00	1.24	6.61	3.45	18.15	6.22	34.96
425	0.00	0.00	1.11	5.49	3.12	15.03	5.73	29.23
300	0.00	0.00	1.02	4.47	2.79	12.25	5.64	23.59
212	0.00	0.00	0.79	3.69	2.28	9.97	4.47	19.12
150	0.00	0.00	0.65	3.04	1.84	8.13	3.61	15.51
106	0.00	0.00	0.60	2.44	1.73	6.40	3.39	12.12
75	0.00	0.00	0.44	1.99	1.29	5.11	2.56	9.57
Pan	0.00		1.99		5.11		9.57	

Table A.14 Results of size analysis for + 13200 – 9500 microns coal

Screen size (microns)	**13200 microns**		**0.5 min**		**1 min**		**2 min**	
	Retained	**Passing**	**Retained**	**Passing**	**Retained**	**Passing**	**Retained**	**Passing**
13200	0.00	100	0.00	100	0.00	100	0.00	100
9500	95.17	4.83	29.31	70.69	12.45	87.55	3.66	96.34
6700	4.48	0.35	22.68	48.01	15.27	72.28	5.77	90.58
4700	0.35	0.00	11.13	36.88	12.52	59.76	6.73	83.84
3350	0.00	0.00	8.17	28.71	9.47	50.29	6.89	76.95
2360	0.00	0.00	5.90	22.81	8.92	41.37	7.85	69.09
1700	0.00	0.00	3.74	19.08	5.97	35.40	7.11	61.99
1180	0.00	0.00	3.77	15.31	6.44	28.96	9.02	52.96
850	0.00	0.00	2.60	12.71	4.47	24.48	7.10	45.86
600	0.00	0.00	2.11	10.60	4.00	20.48	7.32	38.54
425	0.00	0.00	1.82	8.78	3.57	16.91	6.60	31.94
300	0.00	0.00	1.66	7.12	3.31	13.60	6.30	25.64
212	0.00	0.00	1.26	5.86	2.57	11.04	4.88	20.76
150	0.00	0.00	1.02	4.84	2.10	8.94	3.95	16.82
106	0.00	0.00	0.95	3.90	1.91	7.03	3.76	13.05
75	0.00	0.00	0.69	3.20	1.38	5.65	2.69	10.36
Pan	0.00		3.20		5.65		10.36	

Table A.15 Results of size analysis for + 6700 – 4700 microns coal

Screen size (microns)	6700 microns		0.5 min		1 min		2 min	
	Retained	Passing	Retained	Passing	Retained	Passing	Retained	Passing
6700	0.00	100	0.00	100	0.00	100	0.00	100
4700	97.93	2.07	40.90	59.10	18.67	81.33	3.60	96.40
3350	1.73	0.34	21.43	37.66	15.48	65.85	6.61	89.79
2360	0.34	0.00	8.29	29.37	13.70	52.15	9.45	80.34
1700	0.00	0.00	5.92	23.45	8.87	43.28	9.11	71.23
1180	0.00	0.00	5.40	18.06	8.49	34.79	11.20	60.03
850	0.00	0.00	3.50	14.55	5.98	28.81	8.60	51.42
600	0.00	0.00	2.48	12.07	4.96	23.85	8.60	42.82
425	0.00	0.00	2.14	9.93	4.26	19.58	8.19	34.63
300	0.00	0.00	1.90	8.03	3.73	15.85	6.97	27.65
212	0.00	0.00	1.41	6.62	2.93	12.92	4.86	22.79
150	0.00	0.00	1.10	5.52	2.31	10.61	4.21	18.58
106	0.00	0.00	1.03	4.50	2.13	8.48	3.99	14.59
75	0.00	0.00	0.78	3.72	1.56	6.92	2.95	11.63
Pan	0.00		3.72		6.92		11.63	

Table A.16 Results of size analysis for + 3350 – 2360 microns coal

Screen size (microns)	3350 microns		0.5 min		1 min		2 min	
	Retained	Passing	Retained	Passing	Retained	Passing	Retained	Passing
3350	0.00	100	0.00	100	0.00	100	0.00	100
2360	97.64	2.36	41.03	58.97	21.20	78.80	5.56	94.44
1700	1.52	0.84	17.10	41.87	16.37	62.43	9.32	85.11
1180	0.84	0.00	11.11	30.76	15.41	47.02	14.10	71.02
850	0.00	0.00	5.72	25.04	9.01	38.00	10.67	60.34
600	0.00	0.00	4.24	20.80	6.98	31.02	10.53	49.81
425	0.00	0.00	3.19	17.61	5.32	25.70	8.94	40.87
300	0.00	0.00	2.62	14.98	4.69	21.01	8.08	32.80
212	0.00	0.00	1.86	13.13	3.36	17.66	6.01	26.78
150	0.00	0.00	1.50	11.62	2.66	15.00	4.71	22.08
106	0.00	0.00	1.43	10.19	2.47	12.54	4.47	17.60
75	0.00	0.00	1.08	9.11	1.80	10.73	3.23	14.37
Pan	0.00		9.11		10.73		14.37	

Table A.17 Results of size analysis for + 1700 – 1180 microns coal

Screen size (microns)	1700 microns		0.5 min		1 min		2 min	
	Retained	Passing	Retained	Passing	Retained	Passing	Retained	Passing
1700	0.00	100	0.00	100	0.00	100	0.00	100
1180	94.64	5.36	54.24	45.76	36.87	63.13	17.39	82.61
850	4.39	0.97	14.60	31.16	16.47	46.66	14.58	68.03
600	0.97	0.00	6.17	24.99	9.69	36.97	12.57	55.47
425	0.00	0.00	3.91	21.08	6.56	30.41	9.62	45.85
300	0.00	0.00	2.97	18.11	5.27	25.14	8.30	37.55
212	0.00	0.00	1.93	16.19	3.60	21.54	5.83	31.72
150	0.00	0.00	1.49	14.70	2.71	18.83	4.71	27.01
106	0.00	0.00	1.42	13.28	2.44	16.39	4.35	22.66
75	0.00	0.00	1.04	12.24	1.82	14.57	3.20	19.46
Pan	0.00		12.24		14.57		19.46	

Table A.18 Results of size analysis for + 850 – 600 microns coal

Screen size (microns)	850 microns		0.5 min		1 min		2 min	
	Retained	Passing	Retained	Passing	Retained	Passing	Retained	Passing
850	0.00	100	0.00	100	0.00	100	0.00	100
600	96.32	3.68	53.93	46.07	41.66	58.34	27.41	72.59
425	3.11	0.56	17.88	28.19	20.10	38.23	19.85	52.74
300	0.56	0.00	4.52	23.66	7.48	30.76	10.55	42.19
212	0.00	0.00	2.65	21.02	4.46	26.30	6.68	35.51
150	0.00	0.00	2.13	18.89	3.42	22.88	5.13	30.38
106	0.00	0.00	2.12	16.77	3.20	19.68	4.80	25.58
75	0.00	0.00	1.61	15.16	2.37	17.30	3.65	21.93
Pan	0.00		15.16		17.30		21.93	

Table A.19 Results of size analysis for + 300 – 212 microns coal

Screen size (microns)	425 microns		0.5 min		1 min		2 min	
	Retained	Passing	Retained	Passing	Retained	Passing	Retained	Passing
300	0.00	100	0.00	100	0.00	100	0.00	100
212	89.14	10.86	65.86	34.14	54.49	45.51	43.93	56.07
150	10.71	0.15	27.24	6.89	18.79	26.72	20.44	35.62
106	0.15	0.00	4.13	2.77	5.00	21.72	7.58	28.04
75	0.00	0.00	2.07	0.70	2.63	19.10	4.19	23.85
Pan	0.00		0.70		19.10		23.85	

A.2.2 Particle size distributions obtained for the OEM-BSD

Table A.20 Results of size analysis for + 26500 – 22400 microns coal

Screen size (microns)	26500 microns		0.5 min		1 min		2 min	
	Retained	Passing	Retained	Passing	Retained	Passing	Retained	Passing
26500	0.00	100	0.00	100	0.00	100	0.00	100
22400	94.60	5.40	33.87	66.13	16.75	83.25	5.29	94.71
19000	5.40	0.00	20.13	46.00	19.21	64.04	13.41	81.30
16000	0.00	0.00	10.89	35.11	10.80	53.24	11.91	69.39
13200	0.00	0.00	3.15	31.96	5.07	48.17	3.37	66.02
9500	0.00	0.00	6.68	25.29	7.90	40.27	8.21	57.81
6700	0.00	0.00	5.02	20.26	5.88	34.39	5.24	52.57
4700	0.00	0.00	3.07	17.20	4.10	30.29	4.06	48.51
3350	0.00	0.00	2.22	14.98	3.48	26.81	3.56	44.94
2360	0.00	0.00	2.01	12.97	2.90	23.91	3.21	41.74
1700	0.00	0.00	1.44	11.53	2.20	21.71	2.86	38.88
1180	0.00	0.00	1.56	9.97	2.67	19.04	3.66	35.22
850	0.00	0.00	1.15	8.83	1.99	17.06	3.04	32.18
600	0.00	0.00	1.17	7.65	2.19	14.86	3.54	28.63
425	0.00	0.00	1.10	6.55	2.20	12.66	3.76	24.87
300	0.00	0.00	1.07	5.49	2.33	10.34	4.03	20.85
212	0.00	0.00	0.97	4.52	1.89	8.44	3.79	17.06
150	0.00	0.00	0.75	3.77	1.63	6.81	3.03	14.03
106	0.00	0.00	0.70	3.06	1.52	5.29	2.95	11.08
75	0.00	0.00	0.53	2.53	1.15	4.13	2.26	8.82
Pan	0.00		2.53		4.13		8.82	

Table A.21 Results of size analysis for + 19000 – 16000 microns coal

Screen size (microns)	19000 microns		0.5 min		1 min		2 min	
	Retained	Passing	Retained	Passing	Retained	Passing	Retained	Passing
19000	0.00	100	0.00	100	0.00	100	0.00	100
16000	97.16	2.84	25.05	74.95	9.53	90.47	4.15	95.85
13200	2.84	0.00	13.13	61.83	12.21	78.26	5.41	90.44
9500	0.00	0.00	19.78	42.04	15.33	62.93	10.82	79.62
6700	0.00	0.00	11.02	31.02	11.35	51.58	8.86	70.76
4700	0.00	0.00	5.90	25.13	7.51	44.07	6.37	64.39
3350	0.00	0.00	4.34	20.79	6.01	38.06	5.29	59.10
2360	0.00	0.00	3.30	17.48	4.82	33.24	4.92	54.19
1700	0.00	0.00	2.33	15.16	3.78	29.46	4.41	49.78
1180	0.00	0.00	2.50	12.65	4.07	25.39	5.54	44.24

850	0.00	0.00	1.66	10.99	3.02	22.37	4.47	39.77
600	0.00	0.00	1.63	9.36	3.14	19.23	4.88	34.89
425	0.00	0.00	1.46	7.89	2.93	16.30	4.90	29.99
300	0.00	0.00	1.39	6.50	2.98	13.32	5.06	24.93
212	0.00	0.00	1.11	5.38	2.44	10.88	4.49	20.44
150	0.00	0.00	0.85	4.54	1.95	8.94	3.59	16.85
106	0.00	0.00	0.85	3.69	1.84	7.10	3.41	13.45
75	0.00	0.00	0.64	3.06	1.36	5.74	2.65	10.80
Pan	0.00		3.06		5.74		10.80	

Table A.22 Results of size analysis for + 13200 – 9500 microns coal

Screen size (microns)	**13200 microns**		**0.5 min**		**1 min**		**2 min**	
	Retained	**Passing**	**Retained**	**Passing**	**Retained**	**Passing**	**Retained**	**Passing**
13200	0.00	100	0.00	100	0.00	100	0.00	100
9500	98.14	1.86	31.88	68.12	15.47	84.53	6.55	93.45
6700	1.86	0.00	22.11	46.01	18.21	66.32	9.16	84.29
4700	0.00	0.00	12.37	33.64	12.38	53.94	7.97	76.32
3350	0.00	0.00	7.63	26.01	8.95	44.99	7.38	68.94
2360	0.00	0.00	4.94	21.07	7.22	37.76	6.96	61.99
1700	0.00	0.00	3.37	17.70	5.22	32.55	6.12	55.87
1180	0.00	0.00	3.26	14.44	5.22	27.33	7.09	48.78
850	0.00	0.00	2.08	12.36	3.68	23.65	5.63	43.15
600	0.00	0.00	1.94	10.42	3.54	20.10	5.89	37.26
425	0.00	0.00	1.64	8.78	3.21	16.89	5.60	31.66
300	0.00	0.00	1.55	7.23	3.10	13.80	5.54	26.13
212	0.00	0.00	1.23	6.00	2.50	11.30	4.81	21.32
150	0.00	0.00	0.98	5.02	1.99	9.30	3.72	17.60
106	0.00	0.00	0.93	4.08	1.88	7.43	3.52	14.08
75	0.00	0.00	0.70	3.39	1.41	6.02	2.68	11.41
Pan	0.00		3.39		6.02		11.41	

Table A.23 Results of size analysis for + 6700 – 4700 microns coal

Screen size (microns)	**6700 microns**		**0.5 min**		**1 min**		**2 min**	
	Retained	**Passing**	**Retained**	**Passing**	**Retained**	**Passing**	**Retained**	**Passing**
6700	0.00	100	0.00	100	0.00	100	0.00	100
4700	98.34	1.66	34.44	65.56	14.24	85.76	3.93	96.07
3350	1.66	0.00	19.64	45.92	17.12	68.64	7.69	88.38

2360	0.00	0.00	12.62	33.30	13.61	55.02	8.80	79.58
1700	0.00	0.00	7.28	26.02	9.65	45.37	8.44	71.15
1180	0.00	0.00	5.96	20.06	8.99	36.38	10.29	60.85
850	0.00	0.00	3.53	16.53	5.80	30.58	8.03	52.82
600	0.00	0.00	2.98	13.55	5.22	25.36	8.06	44.77
425	0.00	0.00	2.36	11.19	4.33	21.03	7.37	37.40
300	0.00	0.00	2.06	9.13	3.98	17.05	6.83	30.57
212	0.00	0.00	1.53	7.60	3.05	14.00	5.71	24.86
150	0.00	0.00	1.21	6.39	2.34	11.66	4.31	20.55
106	0.00	0.00	1.17	5.22	2.18	9.48	4.03	16.52
75	0.00	0.00	0.91	4.31	1.61	7.87	3.05	13.48
Pan	0.00		4.31		7.87		13.48	

Table A.24 Results of size analysis for + 3350 – 2360 microns coal

Screen size (microns)	**3350 microns**		**0.5 min**		**1 min**		**2 min**	
	Retained	**Passing**	**Retained**	**Passing**	**Retained**	**Passing**	**Retained**	**Passing**
3350	0.00	100	0.00	100	0.00	100	0.00	100
2360	98.83	1.17	47.86	52.14	22.74	77.26	6.38	93.62
1700	1.17	0.00	14.12	38.02	15.78	61.48	9.17	84.45
1180	0.00	0.00	10.54	27.48	14.32	47.16	13.00	71.46
850	0.00	0.00	5.61	21.87	8.59	38.57	10.21	61.25
600	0.00	0.00	4.25	17.63	7.29	31.29	10.00	51.24
425	0.00	0.00	3.13	14.50	5.71	25.57	8.85	42.40
300	0.00	0.00	2.60	11.90	4.95	20.63	7.89	34.50
212	0.00	0.00	1.87	10.03	3.58	17.05	6.29	28.21
150	0.00	0.00	1.46	8.57	2.73	14.32	4.76	23.44
106	0.00	0.00	1.38	7.19	2.51	11.80	4.37	19.07
75	0.00	0.00	1.11	6.08	1.89	9.92	3.33	15.74
Pan	0.00		6.08		9.92		15.74	

Table A.25 Results of size analysis for + 1700 – 1180 microns coal

Screen size (microns)	**1700 microns**		**0.5 min**		**1 min**		**2 min**	
	Retained	**Passing**	**Retained**	**Passing**	**Retained**	**Passing**	**Retained**	**Passing**
1700	0.00	100	0.00	100	0.00	100	0.00	100
1180	97.57	2.43	54.53	45.47	32.96	67.04	14.70	85.30
850	2.03	0.40	13.28	32.19	14.95	52.10	13.19	72.11
600	0.40	0.00	7.25	24.94	11.02	41.07	13.00	59.11
425	0.00	0.00	4.70	20.24	7.79	33.28	10.70	48.41
300	0.00	0.00	3.51	16.73	6.30	26.99	9.26	39.15

212	0.00	0.00	2.31	14.42	4.27	22.72	7.05	32.10
150	0.00	0.00	1.63	12.79	3.12	19.60	5.08	27.02
106	0.00	0.00	1.51	11.28	2.66	16.95	4.61	22.41
75	0.00	0.00	1.19	10.09	1.91	15.04	3.43	18.98
Pan	0.00		10.09		15.04		18.98	

Table A.26 Results of size analysis for + 600 – 425 microns coal

Screen size (microns)	**600 microns**		**0.5 min**		**1 min**		**4 min**	
	Retained	**Passing**	**Retained**	**Passing**	**Retained**	**Passing**	**Retained**	**Passing**
600	0.00	100	0.00	100	0.00	100	0.00	100
425	75.89	24.11	59.22	40.78	49.62	50.38	14.61	85.39
300	20.61	3.50	16.10	24.68	17.75	32.63	17.08	68.30
212	3.50	0.00	3.71	20.97	6.34	26.30	12.50	55.80
150	0.00	0.00	2.18	18.79	2.49	23.81	8.66	47.14
106	0.00	0.00	1.79	17.01	3.05	20.75	7.71	39.43
75	0.00	0.00	1.37	15.63	2.06	18.70	5.86	33.56
Pan	0.00		15.63		18.70		33.56	

B Selection function results for different batch tests

In this section, the values of the different selection functions as calculated from the manipulated data in Tables A.1 to A.26 are presented.

Table B.1 Selection function values for different batch grinding tests

	Selection function (min^{-1})				
Particle size x_i (microns)	**EQM**	**OEM**	**49.2 mm**	**38.8 mm**	**30.6 mm**
26500	1.89	1.15		2.02	
22400			2.71		
19000	2.29	1.52			
16000				2.50	1.08
13200	2.36	1.85			
9500			2.31		1.48
6700	1.68	1.93		2.02	
4700					
3350	1.33	1.47			
2360			1.03	1.11	1.09
1700	0.76	0.94			
1180					
850	0.45				
600		0.39	0.26		
425	0.22				

C Reduced selection function after Snow

This section presents the data that have been used to assess the applicability of Snow's equation (2.14) and the revised equation (2.15) on our results.

C.1 Maximum selection function values for different ball diameters

Table C.1 Particle size corresponding to maximum selection function values for the single sizes of ball

Ball size (mm)	S_m	x_m
30.6	2.50	8.25
38.8	2.94	13.83
49.2	3.52	22.32

C.2 Reduced selection function values

Table C.2 Reduced particle size and selection functions for the single sizes of balls

49.2 mm balls	
S_i/S_m	x_i/x_m
0.77	1.00
0.66	0.43
0.29	0.11
0.07	0.03

38.8 mm balls	
S_i/S_m	x_i/x_m
0.69	1.92
0.85	1.16
0.69	0.48
0.38	0.17

30.6 mm balls	
S_i/S_m	x_i/x_m
0.43	1.94
0.59	1.15
0.44	0.29

D Manipulated data used in the determination of breakage function

In this section, the different results of the reduced breakage functions are presented. The B-II method (Austin *et al.*, 1984) was used to get estimates of the different values of B_{ij} corresponding first to the tests carried out with single ball sizes, then with ball size mixtures. Short grinding times were used, i.e. 0.5 min, and the calculations were done only on particle sizes for which the retained material on the top screen size exceeded 60%.

Table D.1 Breakage function obtained for the single ball sizes

		Normalized					
2360 microns		**49.2 mm balls**		**38.8 mm balls**		**30.6 mm balls**	
Interval index *i*	**Upper size (microns)**	**Size**	B_{ij}	**Size**	B_{ij}	**Size**	B_{ij}
10	**2360**	1.00	1.000	1.00	1.000	1.00	1.000
11	**1700**	0.72	0.662	0.72	0.662	0.72	0.642
12	**1180**	0.50	0.499	0.50	0.499	0.50	0.469
13	**850**	0.36	0.392	0.36	0.391	0.36	0.356
14	**600**	0.25	0.319	0.25	0.218	0.25	0.280
15	**425**	0.18	0.240	0.18	0.288	0.18	0.222
16	**300**	0.13	0.197	0.13	0.197	0.13	0.187
17	**212**	0.09	0.170	0.09	0.170	0.09	0.160
18	**150**	0.06	0.145	0.06	0.145	0.06	0.136
19	**106**	0.05	0.127	0.05	0.127	0.05	0.120

Table D.2 Data used to assess size distributions normalization

Table No.	A11	A16	A17	A18	A19	A24	A25	A26
	Cumulative mass passing (%)							
	Feed size range (mm)							
Screen No.	***0.6/0.425***	***3.35/2.36***	***1.7/1.18***	***0.85/0.6***	***0.425/0.3***	***3.35/2.36***	***1.7/1.18***	***0.6/0.425***
1	100	100	100	100	100	100	100	100
2	48.36	58.97	45.76	46.07	34.14	52.14	45.47	40.78
3	23.91	41.87	31.16	28.19	6.89	38.02	32.19	24.68
4	20.30	30.76	24.99	23.66	2.77	27.48	24.94	20.97
5	18.49	25.04	21.08	21.02	0.70	21.87	20.24	18.79
6	16.89	20.80	18.11	18.89		17.63	16.73	17.01
7	15.72	17.61	16.19	16.77		14.50	14.42	15.63
8		14.98	14.70	15.16		11.90	12.79	
9		13.13	13.28			10.03	11.28	
10		11.62	12.24			8.57	10.09	
11		10.19				7.19		
12		9.11				6.08		

E Prediction of the selection function of ball mixtures

This section presents the summary of the predicted values of the selection function corresponding to the two ball size distributions based upon the material used as characterized in Appendix B and Chapter 4.

E.1 Determination of milling parameters in each ball size interval

Table E.1 Predicted selection function parameters in the different ball intervals used

Index	**Ball size interval (mm)**		***a*** **(min^{-1})**	**μ (mm)**
1	50.0	44.0	0.36	29.4
2	44.0	37.5	0.42	22.1
3	37.5	31.5	0.49	15.8
4	31.5	26.5	0.59	11.2
5	26.5	22.4	0.70	7.9
6	22.4	19.0	0.82	5.7

E.2 Predicted EQM- and OEM-BSD's selection functions

Table E.2 Predicted selection functions for the two ball size distributions and the different ball intervals used

Particle size (mm)	**Ball class index**						**Predictions**	
	1	**2**	**3**	**4**	**5**	**6**	**EQM**	**OEM**
31.5	2.66	1.75	0.91	0.41	0.18	0.08	1.71	1.00
26.5	2.98	2.18	1.23	0.58	0.26	0.12	2.02	1.23
22.4	3.12	2.54	1.60	0.81	0.37	0.17	2.26	1.43
19.0	3.10	2.78	1.97	1.08	0.52	0.23	2.41	1.61
16.0	2.95	2.87	2.30	1.41	0.72	0.34	2.47	1.76
13.2	2.69	2.79	2.53	1.79	1.01	0.50	2.44	1.89
9.5	2.17	2.40	2.52	2.26	1.60	0.91	2.22	1.98
6.7	1.68	1.90	2.15	2.26	2.04	1.46	1.88	1.91
4.7	1.27	1.45	1.69	1.92	2.03	1.85	1.50	1.70
3.35	0.97	1.11	1.31	1.53	1.73	1.82	1.18	1.41
2.36	0.73	0.84	0.99	1.17	1.36	1.54	0.90	1.11
1.7	0.56	0.64	0.76	0.90	1.06	1.23	0.70	0.86
1.18	0.42	0.48	0.57	0.67	0.80	0.93	0.52	0.64

0.85	0.32	0.37	0.43	0.52	0.61	0.72	0.40	0.49
0.6	0.24	0.28	0.33	0.39	0.46	0.54	0.30	0.37
0.425	0.18	0.21	0.25	0.29	0.35	0.41	0.23	0.28
0.3	0.14	0.16	0.19	0.22	0.26	0.31	0.17	0.21

E.3 Statistical analysis of the predictions

This section is based on the book by Triola (2001). Mario F. Triola is a Professor Emeritus of Mathematics at Dutchess Community College, where he has taught statistics for over 30 years. His book was used as a reference for statistical analysis of our data.

Table E.3 Coefficient of determination for the EQM-BSD

			R-squared	0.977
	Selection function values		Mean S_{aver}	1.370
Size x_i [mm]	Measured S_i	Predicted S_{mdl}	$(S_i - S_{aver})^2$	$(S_i - S_{mdl})^2$
26.5	1.89	2.02	0.269	0.018
19	2.29	2.41	0.840	0.015
13.2	2.36	2.44	0.972	0.007
6.7	1.68	1.88	0.093	0.040
3.35	1.33	1.18	0.001	0.023
1.7	0.76	0.70	0.375	0.004
0.85	0.45	0.40	0.852	0.002
0.425	0.22	0.23	1.334	0.000
		Sum	4.736	0.111

Table E.4 Coefficient of determination for the OEM-BSD

			R-squared	0.986
	Selection function values		Mean S_{aver}	1.322
Size x_i [mm]	Measured S_i	Predicted S_{mdl}	$(S_i - S_{aver})^2$	$(S_i - S_{mdl})^2$
26.5	1.153	1.225	0.029	0.005
19	1.522	1.614	0.040	0.008
13.2	1.848	1.886	0.276	0.002
6.7	1.932	1.915	0.373	0.000
3.35	1.469	1.410	0.022	0.003
1.7	0.936	0.860	0.149	0.006
0.6	0.393	0.373	0.863	0.001
		Sum	1.752	0.025